Institute of Physics

Gravitational waves from eccentric binaries

Hansen coefficients and memory effect

Michael Ebersold

Master Thesis

Supervision:

Prof. Dr. Philippe Jetzer
Yannick Boetzel

June 12, 2018

Abstract

In this Master thesis we study gravitational waves from inspiralling eccentric, compact binary systems. The work covers two main topics. In the first part we write the gravitational waveform polarization states using Hansen coefficients. These coefficients have been used to study elliptic motion since 1855 and are defined as the Fourier amplitudes in a series over harmonics of the mean anomaly. We write the waveform polarizations compactly as a sum over Hansen coefficients and give explicit expressions up to first post-Newtonian order. As an application we compute the Fourier transform of the waveform using the stationary phase approximation.

The second part is about the non-linear gravitational wave memory effect. This is a non-oscillatory, slowly-growing contribution to the gravitational wave amplitude, which would cause a permanent displacement of test masses in an ideal, freely-falling gravitational wave detector. The non-linear memory originates from changes in the radiative mass-multipole moments sourced by the gravitational wave energy flux. Although it is a higher order effect, it affects the waveform at leading order due to its hereditary nature, which means that the entire past history of the binary is contributing to the memory. In this work we compute first post-Newtonian corrections to the memory from inspiralling eccentric binaries, thereby extending the leading order calculations done by Favata [1]. In the low eccentricity limit we provide explicit expressions for the memory pieces of the spin-weighted spherical harmonic modes and the waveform polarizations.

Acknowledgments

First of all I want to thank Prof. Dr. Philippe Jetzer for the opportunity to write my Master thesis in his group. It was a pleasure to work in the interesting and thriving field of gravitational waves. I also want to thank Yannick Boetzel for always having answers to my questions and helpful discussions. Moreover, I want to thank the other group members, Dr. Maria Haney and Lionel Philippoz, for providing some useful comments.

Contents

1 Introduction

1.1 Preface

In general relativity, gravity is treated as a phenomenon arising from the curvature of spacetime. The curvature is generated by mass and energy, which are related by the famous formula $E = mc^2$. The connection between curvature of spacetime and mass and energy is beautifully described by Einstein's field equations [2],

$$R_{\mu\nu} - \frac{1}{2} g_{\mu\nu} R = \frac{8\pi G}{c^4} T_{\mu\nu}. \tag{1.1}$$

The left-hand side, including the Ricci tensor $R_{\mu\nu}$ and the Ricci scalar $R = g^{\mu\nu} R_{\mu\nu}$, describes the curvature of spacetime determined by the metric tensor $g_{\mu\nu}$, and the right-hand side describes the matter and energy content in terms of the stress-energy tensor $T_{\mu\nu}$.

Generally, it is difficult to find solutions to the Einstein field equations. There are a few exact solutions for highly symmetrical situations, for example the Schwarzschild solution, which describes spacetime around a spherical, static and non-charged mass distribution [3]. The other possibilities to solve the field equations are to linearize them for weak gravitational fields, to make a systematic expansion for small velocities and weak fields or to rely on numerical methods.

In this thesis we will first give a short overview about gravitational waves. We will show how they appear quite naturally in linearized gravity, explore their polarization states and investigate their quadrupole nature.

In the second part we will write the polarization states of gravitational waves from an inspiralling compact binary system in terms of the long known Hansen coefficients describing elliptic motion.

The third part focuses on a fascinating non-linear effect of general relativity, the gravitational wave memory effect. We will calculate post-Newtonian corrections to the memory from eccentric binaries.

1.1.1 Post-Newtonian expansion

The post-Newtonian (PN) expansion in general relativity is used to find approximate solutions to the Einstein field equations. Based on Newton's law of universal gravitation, general relativistic effects are invoked as small perturbations therefrom. It was Einstein himself who first used this approach to describe the perihelion precession of Mercury [4].

One usually expands the field equations in the small parameter $\frac{v^2}{c^2}$, where v is the velocity of the matter forming the gravitational field and c the speed of light. The power of this parameter gives the respective PN order. One can always set the speed of light to infinity and should recover Newton's law of gravity and the Newtonian equations of motion. When speaking about inspiralling compact binary systems, as we will throughout this thesis, the small parameter is equivalent to $x = \left(\frac{GM\omega}{c^3}\right)^{2/3}$, where M is the total mass of the binary and ω denotes the binaries orbital angular frequency. Note that this parameter is dimensionless and gauge-invariant.

1.1.2 Notation

We will shortly describe some conventions and notation used in this thesis. Usually we will work with geometrized units $G = c = 1$, although sometimes we will explicitly write the gravitational constant G or the speed of light c to indicate dimensions or PN orders.

The flat spacetime metric is assumed to be $\eta_{\mu\nu} = \mathrm{diag}(-1, 1, 1, 1)$. Spacetime indices are denoted with Greek letters $\mu, \nu, ...$ and take values $0, 1, 2, 3$, purely spatial indices are written with Latin letters $i, j, ...$ and take values $1, 2, 3$. Note that spatial indices can be placed arbitrarily ($h_{ij} = h^{ij}$). The Einstein summation convention is always presumed, so a summation over repeated indices in a formula is implied. Sometimes, the following abbreviation for the partial derivative is used: $\partial_\mu A_\nu = A_{\nu,\mu}$. A time derivative can be written with an overdot like $\dot{A}_\mu$ or an upper index in brackets $A_\mu^{(n)}$, indicating the nth-time derivative.

A shorthand notation for symmetrization are brackets $(.)$ around the relevant indices, and for anti-symmetrization square brackets $[.]$. To take the symmetric-trace-free (STF) projection of a tensor, angular brackets $\langle . \rangle$ enclosing the relevant indices are used.

Moreover, our conventions on the n-dimensional Fourier transform are

$$\tilde{F}(k) = \int d^n x \, F(x) e^{-ikx}, \tag{1.2a}$$

$$F(x) = \frac{1}{(2\pi)^n} \int d^n k \, \tilde{F}(k) e^{ikx}, \tag{1.2b}$$

such that for a function of time the metric signature implies

$$\tilde{F}(\omega) = \int dt \, F(t) e^{i\omega t}, \tag{1.3a}$$

$$F(t) = \frac{1}{2\pi} \int d\omega \, \tilde{F}(\omega) e^{-i\omega t}. \tag{1.3b}$$

1.2 Gravitational waves

Since general relativity is a relativistic theory it must be causal. Therefore a change in the local gravitational field can affect a distant observer only after finite time. From this notion, Einstein inferred that gravitational waves must exist [5]. They can be described as ripples in the fabric of spacetime and are generated by accelerated masses. Because gravity is such a weak interaction, it took almost a hundred years until the first gravitational wave signal from a binary black hole merger was recorded in the LIGO gravitational wave detectors on September 14, 2015 [6, 7]. This detection opened up the new branch of gravitational wave astronomy, where information about astrophysical objects and events such as binary neutron stars, binary black holes, supernovae and the Big Bang are searched for in their respective gravitational wave signals. In 2017, Rainer Weiss, Barry Barish and Kip Thorne were awarded the Nobel Prize in Physics "for decisive contributions to the LIGO detector and the observation of gravitational waves" [8].

1.2.1 Linearized gravity

The natural approach to discuss gravitational waves is to work in linearized gravity because they cause only small distortions in spacetime, at least far away from the sources. In linearized gravity one introduces a metric in which the components deviate only slightly from the flat Minkowski metric

$$g_{\mu\nu} = \eta_{\mu\nu} + h_{\mu\nu}, \qquad |h_{\mu\nu}| \ll 1, \tag{1.4}$$

where one calls $h_{\mu\nu}$ the metric perturbation. Employing this metric, we can calculate the Ricci tensor. In doing so, we only keep terms linear in $h_{\mu\nu}$, higher order terms are discarded. As a consequence, covariant derivatives reduce to ordinary derivatives and indices are raised and lowered using the Minkowski metric $\eta_{\mu\nu}$. The linear order Ricci tensor is found to be

$$R_{\mu\nu} = \frac{1}{2}\left(\partial_\rho\partial_\nu h^\rho{}_\mu + \partial_\rho\partial_\mu h^\rho{}_\nu - \Box h_{\mu\nu} - \partial_\mu\partial_\nu h\right), \tag{1.5}$$

where $\Box = \partial_\rho\partial^\rho = -\partial_t^2 + \nabla^2$ is the flat space wave operator and $h = h^\mu{}_\mu$ is the trace of the metric perturbation. Contracting the Ricci tensor gives the Ricci scalar

$$R = R^\mu{}_\mu = \partial_\rho\partial^\mu h^\rho{}_\mu - \Box h. \tag{1.6}$$

It is convenient to make a change from the metric perturbation $h_{\mu\nu}$ to the trace-reversed perturbation $\bar{h}_{\mu\nu} = h_{\mu\nu} - \frac{1}{2}\eta_{\mu\nu}h$. Inserting it into the Ricci tensor and scalar and keeping only linear terms yields for the left-hand side of the field equations

$$R_{\mu\nu} - \frac{1}{2}\eta_{\mu\nu}R = \frac{1}{2}\left(\partial_\rho\partial_\nu\bar{h}^\rho{}_\mu + \partial_\rho\partial_\mu\bar{h}^\rho{}_\nu - \Box\bar{h}_{\mu\nu} - \eta_{\mu\nu}\partial_\rho\partial^\sigma\bar{h}^\rho{}_\sigma\right). \tag{1.7}$$

Since the field equations are generally covariant, we have to choose an appropriate coordinate system or gauge. In general relativity, gauge transformations are just coordinate transformations. Such a transformation of the form $x^{\mu\prime} = x^\mu + \xi^\mu$, where $\xi^\mu(x^\nu)$ is an arbitrary vector field whose derivatives satisfy $|\partial_\mu\xi_\nu| \ll 1$, changes the metric perturbation by

$$h'_{\mu\nu} = h_{\mu\nu} - 2\partial_{(\mu}\xi_{\nu)}, \tag{1.8}$$

and thus the trace-reversed metric by

$$\bar{h}'_{\mu\nu} = \bar{h}_{\mu\nu} - 2\partial_{(\nu}\xi_{\mu)} + \eta_{\mu\nu}\partial^\rho\xi_\rho. \tag{1.9}$$

If one works on radiation related topics, it is usual to choose a Lorenz type gauge, satisfying the condition

$$\partial^\mu\bar{h}_{\mu\nu} = 0. \tag{1.10}$$

This is similar to electrodynamics, where the condition reads $\partial^\mu A_\mu = 0$ and A_μ is the electromagnetic four-potential.

Any metric perturbation can be put into a Lorenz gauge by a coordinate transformation of the form described above that satisfies

$$\Box\xi_\nu = \partial^\mu\bar{h}_{\mu\nu} = 0. \tag{1.11}$$

Applying the gauge condition Eq. (1.10) to the left-hand side of the Einstein field equations Eq. (1.7) will simplify them to

$$R_{\mu\nu} - \frac{1}{2}\eta_{\mu\nu}R = -\frac{1}{2}\Box\bar{h}_{\mu\nu}. \tag{1.12}$$

Therefore the linearized field equations read

$$\Box\bar{h}_{\mu\nu} = -\frac{16\pi G}{c^4}T_{\mu\nu}, \tag{1.13}$$

and in vacuum they reduce to

$$\Box\bar{h}_{\mu\nu} = 0. \tag{1.14}$$

The form of this wave equation is again formally equal to the one describing electromagnetic waves, apart from the fact that we are dealing with a tensor quantity instead of a vector quantity. Besides, one has to keep in mind that in order to get the wave equation derived here, we had to

make approximations, whereas in electromagnetism, the wave equation is exact. The solution to the wave Eq. (1.13) can be obtained using a retarded Green's function in close analogy to electromagnetism. It can be written as

$$\bar{h}_{\mu\nu}(\vec{r},t) = \frac{4G}{c^4}\int d^3r' \frac{T_{\mu\nu}(\vec{r}',t_r)}{|\vec{r}-\vec{r}'|}, \tag{1.15}$$

where $t_r = t - \frac{|\vec{r}-\vec{r}'|}{c}$ is the retarded time. Also the interpretation is straightforward to understand, the disturbance in the gravitational field at $(\vec{r},t)$ is given by the influences from energy and momentum sources at a point $(\vec{r}-\vec{r}',t_r)$ on the past light cone.

1.2.2 TT gauge and polarizations

For the purpose of studying gravitational waves, we specialize to asymptotically flat vacuum spacetimes, thus $h_{\mu\nu} \to 0$ as $r \to \infty$ and $T_{\mu\nu} = 0$ everywhere. In addition to choose the Lorenz gauge, one can further specialize the gauge to make the metric perturbation purely spatial $h_{00} = h_{0i} = h_{i0} = 0$ and traceless $h = h^i{}_i = 0$. This also implies that the spatial metric perturbation is transverse, $\partial^i h_{ij} = 0$. If the metric perturbation is put in this transverse-traceless (TT) gauge, we will write $h^{\mathrm{TT}}_{\mu\nu}$. Furthermore, there is no distinction anymore between $\bar{h}_{\mu\nu}$ and $h_{\mu\nu}$ in the TT gauge due to the tracelessness. It is highly convenient to work with the metric in TT gauge, because it completely fixes the gauge freedom such that $h^{\mathrm{TT}}_{\mu\nu}$ carries only physical information about the radiation. We can define a projection operator Λ_{ijkl} that extracts the TT part of a tensor. It is given by

$$\Lambda_{ijkl} = P_{ik}P_{jl} - \frac{1}{2}P_{ij}P_{kl}, \tag{1.16}$$

where $P_{ij} = \delta_{ij} - N_iN_j$.

Likewise, in TT gauge it is straightforward to show that gravitational waves have two polarizations. Suppose a gravitational wave propagating in z-direction, then $h^{\mathrm{TT}}_{ij} = h^{\mathrm{TT}}_{ij}(t-z)$ is a solution to the wave equation $\Box h^{\mathrm{TT}}_{ij} = 0$. Because of the Lorenz gauge condition $\partial_z h^{\mathrm{TT}}_{zj} = 0$, $h^{\mathrm{TT}}_{zj}(t-z)$ must be a constant and in order to satisfy the condition that $h_{\mu\nu} \to 0$ as $r \to \infty$ this constant must be zero. The non-zero components of h^{TT}_{ij} are therefore h^{TT}_{xx}, h^{TT}_{yy}, h^{TT}_{xy} and h^{TT}_{yx}. Symmetry and the trace-free condition impose two more relations, such that we are left with two independent components

$$h^{\mathrm{TT}}_{xx} = -h^{\mathrm{TT}}_{yy} = h_+(t-z), \tag{1.17a}$$
$$h^{\mathrm{TT}}_{xy} = h^{\mathrm{TT}}_{yx} = h_\times(t-z). \tag{1.17b}$$

These are the two waveform polarizations which comprise the plus- and the cross-polarization. In Fig. 1.1 (taken from Ref. [9]) the two polarization states are illustrated.

1.2.3 Quadrupole radiation

We will now consider gravitational radiation emitted by a distant, isolated source of non-relativistic matter. This will lead us to the famous quadrupole formula already developed by Einstein [10].

First we take the Fourier transform of the metric perturbation with respect to time and insert the general solution (Eq. (1.15)) while changing the integration variable from t_r to t. Using once again the definition of the Fourier transform leads to

$$\begin{aligned}\tilde{\bar{h}}_{\mu\nu}(\vec{r},\omega) &= \int dt\, e^{i\omega t}\bar{h}_{\mu\nu}(\vec{r},t) \\ &= 4G\int dt_r\, d^3r'\, e^{i\omega|\vec{r}-\vec{r}'|}\, e^{i\omega t_r}\frac{T_{\mu\nu}(\vec{r}',t_r)}{|\vec{r}-\vec{r}'|}\end{aligned}$$

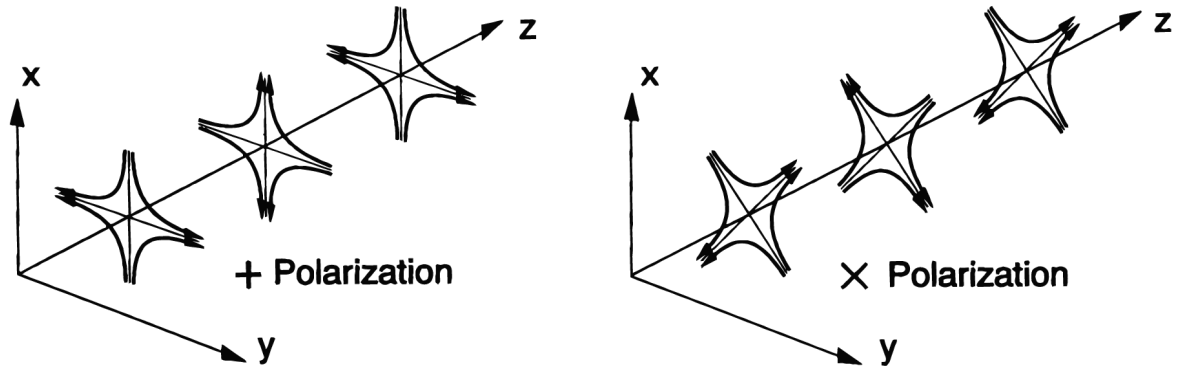

Figure 1.1: The lines of force for the two polarization states of gravitational waves are shown for a wave propagating in z-direction. The one on the left is purely in the plus-polarization state while the wave on the right is purely cross-polarized. In both cases the excitations are only in the plane perpendicular to the direction of propagation. (Figure from Ref. [9])

$$= 4G \int d^3r' \, e^{i\omega|\vec{r}-\vec{r}'|} \frac{\tilde{T}_{\mu\nu}(\vec{r}', \omega)}{|\vec{r}-\vec{r}'|}. \tag{1.18}$$

Employing the fact that the size of the source is small compared to the distance to the observer, we can make the approximation $|\vec{r}-\vec{r}'| \approx r$ and write the Fourier transform of the metric perturbation as

$$\tilde{\bar{h}}_{\mu\nu}(\vec{r}, \omega) = 4G \frac{e^{i\omega r}}{r} \int d^3r' \, \tilde{T}_{\mu\nu}(\vec{r}', \omega). \tag{1.19}$$

We only need to compute the spatial components of $\tilde{\bar{h}}_{\mu\nu}(\vec{r}, \omega)$ because the Lorenz gauge condition (Eq. (1.10)) in Fourier space relates the timelike indices to the spatial ones via

$$\tilde{\bar{h}}^{0\nu} = \frac{i}{\omega} \partial_i \tilde{\bar{h}}^{i\nu}. \tag{1.20}$$

Hence, for the evaluation of Eq. (1.19) we take the spatial part of $\tilde{T}_{\mu\nu}(\vec{r}, \omega)$ and integrate it by parts

$$\int d^3r \, \tilde{T}^{ij}(\vec{r}, \omega) = \int d^3r \, \partial_k (x^i \tilde{T}^{kj}) - \int d^3r \, x^i (\partial_k \tilde{T}^{kj}), \tag{1.21}$$

where the first term is a surface integral which vanishes because the source is isolated. The second term can be rewritten using the Fourier-space version of the conservation of the stress-energy tensor $-\partial_k \tilde{T}^{k\mu} = i\omega \tilde{T}^{0\mu}$. We continue as follows

$$\begin{aligned}
\int d^3r \, \tilde{T}^{ij}(\vec{r}, \omega) &= i\omega \int d^3r \, x^i \tilde{T}^{0j} \\
&= \frac{i\omega}{2} \int d^3r \left(x^i \tilde{T}^{0j} + x^j \tilde{T}^{0i} \right) \\
&= \frac{i\omega}{2} \int d^3r \left[\partial_k \left(x^i x^j \tilde{T}^{0k} \right) - x^i x^j \left(\partial_k \tilde{T}^{0k} \right) \right] \\
&= -\frac{\omega^2}{2} \int d^3r \, x^i x^j \tilde{T}^{00}.
\end{aligned} \tag{1.22}$$

In the second line we have used the fact that the left-hand side is symmetric in i and j. Then we performed again integration by parts and have used the conservation of $T^{\mu\nu}$. Since T^{00} is nothing else than the energy density, we can recognize the quadrupole moment tensor in the last

line of Eq. (1.22) which is defined by

$$I_{ij}(t) = \int d^3r\, x^i x^j T^{00}(\vec{r}, t). \tag{1.23}$$

Therefore we can write the spatial part of the Fourier transform of the metric given in Eq. (1.19) in terms of the Fourier transform of the quadrupole tensor

$$\tilde{\bar{h}}_{ij}(\vec{r}, \omega) = -2G\omega^2 \frac{e^{i\omega r}}{r} \tilde{I}_{ij}(\omega). \tag{1.24}$$

Transforming this result back to t we find the quadrupole formula

$$\bar{h}_{ij}(\vec{r}, t) = \frac{2G}{r} \frac{d^2 I_{ij}}{dt^2}(t_r). \tag{1.25}$$

For gravitational waves, the leading order contribution comes from changes in the quadrupole moment of the energy density. This is in contrast to electromagnetic radiation, where the leading contribution comes from the changing dipole moment of the charge density. A changing dipole moment corresponds to the motion of the density center. Nothing prevents the center of an electromagnetic charge density from oscillating, whereas an oscillation of the center of mass in an isolated system would violate momentum conservation.

1.2.4 Energy loss due to gravitational radiation

In general, there is no true local measure of the energy in the gravitational field. However, in the weak field limit it is possible to find a stress-energy tensor for the metric perturbations $h_{\mu\nu}$, representing the energy in gravitational waves. To do so, we study the vacuum field equations $R_{\mu\nu} = 0$ at second order. Expanding the metric and the Ricci tensor to second order,

$$g_{\mu\nu} = \eta_{\mu\nu} + h^{(1)}_{\mu\nu} + h^{(2)}_{\mu\nu}, \tag{1.26a}$$

$$R_{\mu\nu} = R^{(0)}_{\mu\nu} + R^{(1)}_{\mu\nu} + R^{(2)}_{\mu\nu}, \tag{1.26b}$$

the first and second order vacuum equations are of the form

$$R^{(1)}_{\mu\nu}[h^{(1)}] = 0, \tag{1.27a}$$

$$R^{(1)}_{\mu\nu}[h^{(2)}] + R^{(2)}_{\mu\nu}[h^{(1)}] = 0, \tag{1.27b}$$

where the notation $R^{(1)}_{\mu\nu}[h^{(2)}]$ means to take the linear order Ricci tensor given in Eq. (1.5) but invoke the second order perturbation $h^{(2)}_{\mu\nu}$. The term $R^{(2)}_{\mu\nu}[h^{(1)}]$ denotes the quadratic part of the Ricci tensor given by

$$\begin{aligned} R^{(2)}_{\mu\nu} = {} & \frac{1}{2} h^{\rho\sigma} \partial_\mu \partial_\nu h_{\rho\sigma} + \frac{1}{4} (\partial_\mu h_{\rho\sigma}) \partial_\nu h^{\rho\sigma} + (\partial^\sigma h^\rho{}_\nu) \partial_{[\sigma} h_{\rho]\mu} - h^{\rho\sigma} \partial_\rho \partial_{(\mu} h_{\nu)\sigma} \\ & + \frac{1}{2} \partial_\sigma (h^{\rho\sigma} \partial_\rho h_{\mu\nu} - \frac{1}{4} (\partial_\rho h_{\mu\nu}) \partial^\rho h - (\partial_\sigma h^{\rho\sigma} - \frac{1}{2} \partial^\rho h) \partial_{(\mu} h_{\nu)\rho}, \end{aligned} \tag{1.28}$$

applied to the first order metric perturbation $h^{(1)}_{\mu\nu}$. At this point we rewrite the second order field equations from the form $R_{\mu\nu} = 0$ to $R_{\mu\nu} - \frac{1}{2}\eta_{\mu\nu} R = 0$. In doing so, we take the terms involving the second order Ricci tensor to the right-hand side and label them as a stress-energy tensor, thus

$$R^{(1)}_{\mu\nu}[h^{(2)}] - \frac{1}{2} \eta^{\rho\sigma} R^{(1)}_{\rho\sigma}[h^{(2)}] \eta_{\mu\nu} = 8\pi G t_{\mu\nu}, \tag{1.29}$$

where we have defined

$$t_{\mu\nu} = -\frac{1}{8\pi G} \left(R^{(2)}_{\mu\nu}[h^{(1)}] - \frac{1}{2} \eta^{\rho\sigma} R^{(2)}_{\rho\sigma}[h^{(1)}] \eta_{\mu\nu} \right). \tag{1.30}$$

This expression can be recognized as the gravitational wave stress-energy tensor. Due to the Bianchi identity, it must be conserved in the background flat space, $\partial_\mu t^{\mu\nu} = 0$. A problem that arises is that $t_{\mu\nu}$ is not gauge invariant. One way to resolve this problem is to average the stress-energy tensor over several wavelengths, which we denote by angle brackets $\langle . \rangle$.

We are now able to calculate an explicit form of the stress-energy tensor defined in Eq. (1.30) in terms of the metric perturbation using the expression for the second order Ricci tensor Eq. (1.28). This calculation is a mess, details can be found for example in the book of Carroll [11]. To simplify the expressions, it is normally carried out in the transverse-traceless gauge. At the end one finds:

$$t_{\mu\nu} = \frac{1}{32\pi G} \Big\langle \left(\partial_\mu h^{\mathrm{TT}}_{\rho\sigma}\right) \left(\partial_\nu h^{\rho\sigma}_{\mathrm{TT}}\right) \Big\rangle. \tag{1.31}$$

Note that one often writes the metric perturbations in $t_{\mu\nu}$ using purely spatial indices, since in TT gauge the time components vanish $h^{\mathrm{TT}}_{0\nu} = 0$.

We now want to calculate the rate of energy loss of a system emitting gravitational waves according to the quadrupole formula Eq. (1.25). The total amount of energy in gravitational radiation in a given volume is

$$E = \int d^3x \, t_{00}, \tag{1.32}$$

and the total energy radiated to infinity is

$$\Delta E = \int dt \, P, \tag{1.33}$$

where P is the power given by

$$P = \int d\Omega \, r^2 t_{0\mu} n^\mu. \tag{1.34}$$

The normal vector n^μ is orthogonal to the surface of the sphere and is therefore the radial unit vector in spherical coordinates. Thus, the relevant part of the gravitational wave stress-energy tensor is t_{0r}. It is often more convenient to define the reduced quadrupole moment

$$Q_{ij} = I_{ij} - \frac{1}{3}\delta_{ij}\delta^{kl} I_{kl}, \tag{1.35}$$

which is the traceless part of I_{ij} (Eq. (1.23)). Since we are interested in the transverse-traceless part of h^{TT}_{ij}, the quadrupole formula still reads

$$h^{\mathrm{TT}}_{ij} = \frac{2G}{r} \frac{d^2 Q^{\mathrm{TT}}_{ij}}{dt^2}(t_r). \tag{1.36}$$

The quadrupole moment depends only on the retarded time $t_r = t - r$, so to calculate t_{0r} according to Eq. (1.31) we need the expressions

$$\partial_0 h^{\mathrm{TT}}_{ij} = \frac{2G}{r} \frac{d^3 Q^{\mathrm{TT}}_{ij}}{dt^3}, \tag{1.37a}$$

$$\partial_r h^{\mathrm{TT}}_{ij} = -\frac{2G}{r} \frac{d^3 Q^{\mathrm{TT}}_{ij}}{dt^3} - \frac{2G}{r^2} \frac{d^2 Q^{\mathrm{TT}}_{ij}}{dt^2}, \tag{1.37b}$$

where we will drop the r^{-2} term since we are in the radiation zone far away from the source. For the relevant part of the gravitational wave stress energy tensor we therefore find

$$t_{0r} = -\frac{G}{8\pi r^2} \left\langle \left(\frac{d^3 Q^{\mathrm{TT}}_{ij}}{dt^3}\right) \left(\frac{d^3 Q^{ij}_{\mathrm{TT}}}{dt^3}\right) \right\rangle. \tag{1.38}$$

Converting this expression back to non-transverse-traceless form, which involves some messy algebra, and evaluating the angular integral in Eq. (1.34), the expression for the power becomes

$$P = -\frac{G}{5}\left\langle \frac{d^3Q_{ij}}{dt^3}\frac{d^3Q^{ij}}{dt^3}\right\rangle. \tag{1.39}$$

Since this formula represents the rate at which the energy is changing, the minus sign indicates that radiating sources are losing energy.

1.2.5 Coordinate system choice

Here we describe the coordinate system and define the polarization triad with which we will work in the following chapters. We first establish an asymptotically-flat radiative coordinate system (T, X, Y, Z) where $(\vec{e}_X, \vec{e}_Y, \vec{e}_Z)$ are spatial orthonormal basis vectors. The corresponding spherical coordinate system is (T, R, Θ, Φ). In both systems the center-of-mass of the source marks the origin. If the source is a binary system, the angular momentum points along the Z-axis and ϕ is an angle in the orbital plane measured from the positive X-axis.

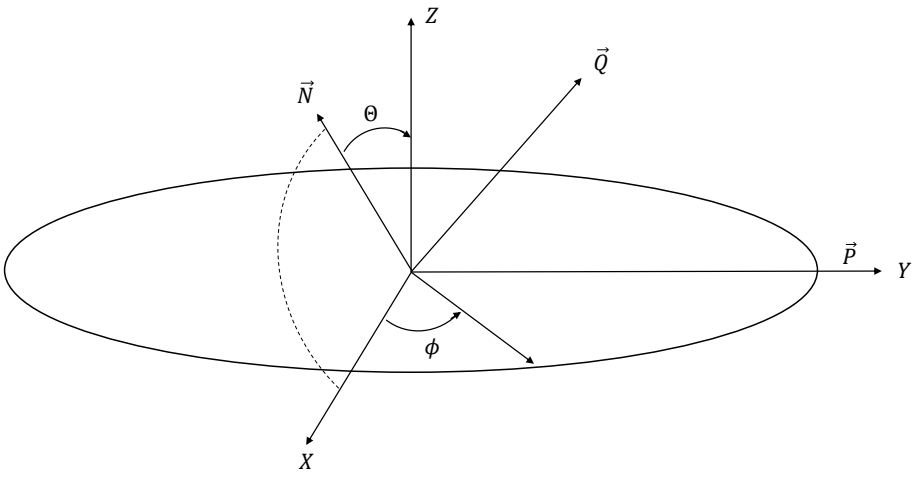

Figure 1.2: Orientation of unit vectors $\vec{N}, \vec{P}, \vec{Q}$ defining the plus- and cross-polarization waveforms in the radiative coordinate system (X, Y, Z). The binary's Newtonian angular momentum defines the Z-axis and ϕ is an angle in the orbital plane, measured from the positive X-axis in a counterclockwise sense. The angle between the direction to the observer $\vec{N}$ and the Z-axis is the inclination angle Θ.

When computing the independent polarization states of gravitational waves emitted by binary systems, one needs to choose a convention for the orientation and direction of the orbit. Following Refs. [12, 13] we choose a triad of unit vectors $(\vec{N}, \vec{P}, \vec{Q})$. $\vec{N}$ points from the origin to the observer, it is given by $\vec{N} = \vec{R}/R$ where R is the radial distance from the source to the observer. The angle between Z-axis and $\vec{N}$ is the inclination angle Θ of the orbital plane. The unit vector $\vec{P}$ lies along the line of nodes and coincides with the Y-axis and $\vec{Q}$ is defined by $\vec{Q} = \vec{N} \times \vec{P}$. An illustration is given in Fig. 1.2.

The plus- and cross-polarization states of gravitational waves are then calculated from the TT piece of the metric perturbation as follows:

$$h_+ = \frac{1}{2}\left(P_i P_j - Q_i Q_j\right) h_{ij}^{\mathrm{TT}}, \tag{1.40a}$$

$$h_\times = \frac{1}{2}\left(P_i Q_j + P_j Q_i\right) h_{ij}^{\mathrm{TT}}. \tag{1.40b}$$

Since $\vec{N}$ is given by the direction to the observer, it is quite natural to choose for the remaining unit vectors: $\vec{P} = \vec{e}_\Theta$ and $\vec{Q} = \vec{e}_\Phi$. Note that this choice is not unique and there exist different conventions.

2 Gravitational wave polarizations in terms of Hansen coefficients

The goal of this chapter is to express the waveform of an eccentric binary inspiral in terms of the long known Hansen coefficients. First, we describe how the orbital motion is parametrized in the post-Newtonian formalism. Second, we derive explicit expressions for the Hansen coefficients valid up to 3PN order. Third, we write the gravitational wave polarizations with these Hansen coefficients and finally we show how to invoke radiation-reaction and a possibility to transform the waveform analytically into frequency space.

2.1 Orbital dynamics

2.1.1 Classical Keplerian parametrization

The Newtonian orbital dynamics of a two-body system in an eccentric orbit is specified by the following parametrization of the components of the separation vector $\vec{r} = r(\cos\phi, \sin\phi)$

$$r = a(1 - e\cos u), \tag{2.1a}$$

$$\phi - \phi_0 = v = 2\arctan\left(\sqrt{\frac{1+e}{1-e}}\tan\frac{u}{2}\right). \tag{2.1b}$$

Here the angles u and v describe eccentric and true anomaly. The ellipse is further described by the semi-major axis a, the eccentricity e and some initial angle ϕ_0. The famous Kepler equation

$$l = n(t - t_0) = u - e\sin u, \tag{2.2}$$

links the mean anomaly l to the eccentric anomaly u and determines the temporal evolution of the auxiliary angles. The mean motion n is given by the orbital period P as $n = 2\pi/P$ and t_0 is some initial time. Since the orbital motion is fully conservative, the orbital elements a, e and n can be written in terms of the orbital energy per reduced mass E and the orbital angular momentum per reduced mass J, the reduced mass being $\mu = m_1 m_2/M$ where m_1 and m_2 are the masses of the individual components of the binary and $M = m_1 + m_2$ their sum:

$$a = -\frac{GM}{2E}, \tag{2.3a}$$

$$e^2 = 1 + \frac{2EJ^2}{G^2M^2}, \tag{2.3b}$$

$$n = \frac{(-2E)^{3/2}}{GM}. \tag{2.3c}$$

One way to solve the Kepler equation Eq. (2.2) is by writing $u - l$ as a Fourier Series and invoking Bessel functions of the first kind J_s in the computation of the Fourier coefficients (see for example Eq. (6) in Ref. [14]). The eccentric anomaly can then be written in terms of the mean anomaly as

$$u = l + \sum_{s=1}^{\infty} \frac{2}{s} J_s(se)\sin(sl). \tag{2.4}$$

2.1.2 PN-accurate quasi-Keplerian parametrization

The most popular approach to incorporate general-relativistic corrections to the dynamics of compact binaries is the post-Newtonian approximation. Currently, the dynamics have been computed to fourth post-Newtonian order [15]. Surprisingly, it is possible to keep the parametrization in a Keplerian form when going to higher orders, at least up to the third post-Newtonian order. At 3PN order the parametrization is given by:

$$r = a_r(1 - e_r \cos u), \tag{2.5a}$$

$$\phi - \phi_0 = (1+k)v + (f_{4\phi} + f_{6\phi})\sin(2v) + (g_{4\phi} + g_{6\phi})\sin(3v) + i_{6\phi}\sin(4v) + h_{6\phi}\sin(5v), \tag{2.5b}$$

$$v = 2\arctan\left(\sqrt{\frac{1+e_\phi}{1-e_\phi}}\tan\frac{u}{2}\right), \tag{2.5c}$$

$$l = u - e_t \sin u + (g_{4t})(v-u) + (f_{4t} + f_{6t})\sin v + i_{6t}\sin(2v) + h_{6t}\sin(3v). \tag{2.5d}$$

The eccentricity now splits in a radial, angular and time eccentricity (e_r, e_ϕ, e_t), a_r is some PN-accurate semimajor axis and k provides the rate of periastron advance per orbital revolution. These orbital elements appear at 1PN order. At 2PN and 3PN order some more orbital functions $g_{4\phi}$, $g_{6\phi}$, $f_{4\phi}$, $f_{6\phi}$, $i_{6\phi}$, $h_{6\phi}$, g_{4t}, g_{6t}, f_{4t}, f_{6t}, i_{6t} and h_{6t} are necessary. All those orbital functions can be written in terms of orbital energy and angular momentum, 3PN-accurate explicit expressions are given in Ref. [16].

Writing the orbital dynamics of an eccentric two-body system in the above form is usually referred to as the "generalized quasi-Keplerian" parametrization. An elegant solution to the 3PN-accurate Kepler equation (Eq. (2.5d)) is derived in Ref. [14].

2.2 Hansen coefficients

2.2.1 Definition

The Hansen coefficients are an important tool in analytical methods of celestial mechanics and are known since the middle of the 19th century [17]. They are used to describe elliptic orbits in form of an expansion. The Hansen coefficients $X_k^{n,m}$ are defined as the Fourier coefficients in the series

$$\left(\frac{r}{a}\right)^n e^{imv} = \sum_{k=-\infty}^{\infty} X_k^{n,m} e^{ikl}, \tag{2.6}$$

where r is the radial distance, a is the semi-major axis of the ellipse, n and m are integer numbers and v and l are the true and mean anomaly, respectively. These coefficients can be computed by the Fourier integral

$$X_k^{n,m} = \frac{1}{2\pi}\int_{-\pi}^{\pi} dl \left(\frac{r}{a}\right)^n e^{imv} e^{-ikl}. \tag{2.7}$$

A method to compute this integral can for example be found in Ref. [18]. Various work has been done concerning the Hansen coefficients, a selection includes the generalization to real n [19], their analytic properties [20] or their efficient computation [21, 22, 23].

Why are we interested in the Hansen coefficients, when talking about gravitational waves? The reason is that the gravitational wave polarizations can be expressed as a linear combination of terms of the form

$$\frac{e^{iju}e^{im\phi}}{r^n}. \tag{2.8}$$

Therefore the Hansen coefficients should appear if the gravitational wave polarizations are written in terms of the mean anomaly l.

2.2.2 Newtonian Hansen coefficients

The goal is to compute the Hansen coefficients, which at Newtonian order are just functions of the eccentricity e. To do this, we start by inserting the radial distance, given in the Keplerian parametrization as Eq. (2.1a), in the left-hand side of the definition of the Hansen coefficients Eq. (2.6),

$$\left(\frac{r}{a}\right)^n e^{imv} = (1 - e\cos u)^n \, e^{imv}. \tag{2.9}$$

The task is now to write this equation as a Fourier series in terms of the mean anomaly l. In this form we will be able to recognize the Hansen coefficients.

We start with the term $(1 - e\cos u)^n$. According to Eq. (41a) of Ref. [14], this expression can be expanded in a Fourier series over u as

$$(1 - e\cos u)^n = \sum_{j=0}^{\infty} b_j^{-n} \cos(ju), \tag{2.10}$$

where the coefficients b_j^n are expressions involving the hypergeometric function ${}_2F_1$ and are explicitly given in Appendix A. This series expansion is carefully derived in Ref. [24] and is valid for negative n. This is not a problem since we are expecting only Hansen coefficients with a negative n to appear in the expressions for the waveform polarization states.

Since we want the whole expression as a Fourier series in terms of the mean anomaly l, we can use the Kepler equation to find a Fourier series expansion for $\cos(ju)$. This has been computed in Eq. (29) of Ref. [14] and reads

$$\cos(ju) = \sum_{s=0}^{\infty} \zeta_s^{ju} \cos(sl), \tag{2.11}$$

explicit expressions for the coefficients ζ_s^{ju} are provided in Appendix A. The resulting series expansion of $(1 - e\cos u)^n$ is therefore

$$(1 - e\cos u)^n = \sum_{j=0}^{\infty} \mathcal{A}_j^{-n} \cos(jl), \tag{2.12a}$$

$$\mathcal{A}_j^n = \sum_{k=0}^{\infty} b_k^n \zeta_j^{ku}. \tag{2.12b}$$

The next step is to write the e^{imv} part of Eq. (2.9) in terms of l. Expanding in a Fourier series we have

$$e^{imv} = \sum_{s=-\infty}^{\infty} \epsilon_s^{mv} e^{isl}, \tag{2.13a}$$

where the coefficients ϵ_s^{mv} come from relating true and eccentric anomaly and are themselves given by a series,

$$\epsilon_s^{mv} = \sum_{k=0}^{\infty} \mathcal{E}_k^m \epsilon_s^{ku}. \tag{2.13b}$$

The coefficients $\mathcal{E}_k^m$ are as well just functions of the eccentricity, explicit expressions can be found in Appendix A.

At this point, we are in the position to put together Eqs. (2.12a) and (2.13a) and write them as a single series over e^{ikl},

$$(1 - e\cos u)^n \, e^{imv} = \left(\sum_{j=0}^{\infty} \mathcal{A}_j^{-n} \cos(jl)\right) \left(\sum_{s=-\infty}^{\infty} \epsilon_s^{mv} e^{isl}\right)$$

$$
\begin{aligned}
&= \left(\sum_{j=-\infty}^{\infty} \frac{1}{2} \mathcal{A}_{|j|}^{-n} e^{ijl} + \frac{\mathcal{A}_0^{-n}}{2} \right) \left(\sum_{s=-\infty}^{\infty} \epsilon_s^{mv} e^{isl} \right) \\
&= \sum_{j=-\infty}^{\infty} \sum_{s=-\infty}^{\infty} \frac{1}{2} \mathcal{A}_{|j|}^{-n} \left(1 + \delta_{j0}\right) \epsilon_s^{mv} e^{i(s+j)l} \\
&= \sum_{k=-\infty}^{\infty} \sum_{j=-\infty}^{\infty} \frac{1}{2} \mathcal{A}_{|j|}^{-n} \left(1 + \delta_{j0}\right) \epsilon_{k-j}^{mv} e^{ikl}. \qquad (2.14)
\end{aligned}
$$

In the second line we have converted the cosine series to an exponential one and afterwards brought together the exponential terms and introduced a new summation index $k = s + j$. Looking at the definition of the Hansen coefficients

$$
(1 - e\cos u)^n e^{imv} = \sum_{k=-\infty}^{\infty} X_k^{n,m} e^{ikl}, \qquad (2.15)
$$

we can read off the $X_k^{n,m}$ of Eq. (2.14) and find

$$
\begin{aligned}
X_k^{n,m} &= \sum_{j=-\infty}^{\infty} \frac{1}{2} \mathcal{A}_{|j|}^{-n} \left(1 + \delta_{j0}\right) \epsilon_{k-j}^{mv} \\
&= \frac{1}{2} \sum_{j=-\infty}^{\infty} \sum_{p=0}^{\infty} \sum_{q=0}^{\infty} \left(b_p^{-n} \zeta_{|j|}^{pu} - \frac{e}{2} b_1^{-n} \delta_{j0} \right) \mathcal{E}_q^m \epsilon_{k-j}^{qu}, \qquad (2.16)
\end{aligned}
$$

where in the last line we have reinserted the series expansion given in Eqs. (2.12b) and (2.13b).

To check the correctness of our formula, we calculate some Hansen coefficients explicitly, perform a Taylor expansion in eccentricity and compare the result to another method to calculate the Hansen coefficients presented in Ref. [18]. They provide an explicit formula as a power series in $\beta = \left(1 - \sqrt{1 - e^2}\right)/e$ and coefficients involving Bessel functions, which reads

$$
X_k^{n,m} = (1 + \beta^2)^{-n-1} \sum_{s=0}^{s_1} \left[\sum_{j=-s}^{j_1} \binom{n - m + 1}{s} \binom{n + m + 1}{s + j} (-\beta)^j J_{k-m+j}(ke) \right] \beta^{2s}, \qquad (2.17a)
$$

where s_1 and $j_1 = t_1 - s_1$ are given by

$$
s_1 = \begin{cases} n - m + 1 & \text{if} \quad n - m + 1 \geq 0 \\ \infty & \text{if} \quad n - m + 1 < 0 \end{cases}, \qquad (2.17b)
$$

$$
t_1 = \begin{cases} n + m + 1 & \text{if} \quad n + m + 1 \geq 0 \\ \infty & \text{if} \quad n + m + 1 < 0 \end{cases}. \qquad (2.17c)
$$

As an example we provide the Hansen coefficients $X_2^{-2,2}$ and $X_{-1}^{-3,4}$ expanded in eccentricity up to $\mathcal{O}(e^{12})$. Both formulas, Eq. (2.16) and Eq. (2.17), yield the same result:

$$
X_2^{-2,2} = 1 - \frac{7}{2}e^2 + \frac{29}{16}e^4 - \frac{53}{288}e^6 + \frac{19}{288}e^8 + \frac{923}{28800}e^{10} + \frac{207871}{8294400}e^{12}, \qquad (2.18a)
$$

$$
X_{-1}^{-3,4} = \frac{11}{3840}e^5 + \frac{407}{92160}e^7 + \frac{4979}{1032192}e^9 + \frac{333757}{70778880}e^{11}. \qquad (2.18b)
$$

2.2.3 Post-Newtonian Hansen coefficients

In the Newtonian case, the orbital phase ϕ reduces to the true anomaly v (Eq. (2.5c)). At first post-Newtonian order, the periastron advance k comes in and at higher PN orders terms proportional to $\sin(mv)$ appear in the expression for ϕ (Eq. (2.5b)).

Due to the periastron advance, ϕ is clearly not 2π-periodic anymore. This suggests the split of ϕ into a term $W(l)$ that is still 2π-periodic in l and a term linear in l, given by λ:

$$\phi = \lambda + W(l), \tag{2.19a}$$

$$\lambda = \phi_0 + (1+k)l, \tag{2.19b}$$

$$\begin{aligned} W(l) = {} & (1+k)(v-l) + (f_{4\phi} + f_{6\phi})\sin(2v) \\ & + (g_{4\phi} + g_{6\phi})\sin(3v) + i_{6\phi}\sin(4v) + h_{6\phi}\sin(5v). \end{aligned} \tag{2.19c}$$

We can now write $e^{im\phi}$ with a term 2π-periodic in l (orbital motion) and one 2π-periodic in the much longer periastron advance timescale,

$$\begin{aligned} e^{im\phi} &= e^{im\lambda} e^{imW} \\ &= e^{iml} e^{imkl} e^{imW} \\ &= e^{im\delta l} e^{iml} e^{imW}. \end{aligned} \tag{2.20}$$

In the last line we introduced the parameter $\delta l = kl$, so that the timescales are clearly separated.

In going to the post-Newtonian framework, the left-hand side of Eq. (2.15) is generalized from $(1 - e\cos u)^n e^{imv}$ to $(1 - e_r \cos u)^n e^{im\phi}$. Therefore in the series expansion of the first term, the radial eccentricity e_r appears

$$(1 - e_r \cos u)^n = \sum_{j=0}^{\infty} b_j^{-n} \cos(ju), \tag{2.21}$$

such that also the coefficients b_j^n are functions of e_r. The further coefficients coming from the series expansion of $\cos(ju)$ are still functions of the time eccentricity e_t, since u and l are related via the Kepler equation (Eq. (2.5d)).

The Fourier series expansion of the e^{imW} term,

$$e^{imW} = \sum_{s=-\infty}^{\infty} \mathcal{P}_s^{mW} e^{isl}, \tag{2.22}$$

invokes more coefficients $\mathcal{P}_s^{mW}$, they are thoroughly derived in Appendix E of Ref. [14]. Inserting all series expansion and performing the same steps as in the Newtonian case we find:

$$\begin{aligned} (1 - e_r \cos u)^n \, e^{im\phi} &= (1 - e_r \cos u)^n e^{imW} e^{iml} e^{im\delta l} \\ &= \left(\sum_{j=0}^{\infty} \mathcal{A}_j^{-n} \cos(jl) \right) \left(\sum_{s=-\infty}^{\infty} \mathcal{P}_s^{mW} e^{isl} \right) e^{iml} e^{im\delta l} \\ &= \sum_{s=-\infty}^{\infty} \sum_{j=-\infty}^{\infty} \frac{1}{2} \mathcal{A}_{|j|}^{-n} \left(1 + \delta_{j0}\right) \mathcal{P}_s^{mW} e^{i(j+s+m)l} e^{im\delta l} \\ &= \sum_{k=-\infty}^{\infty} \sum_{j=-\infty}^{\infty} \frac{1}{2} \mathcal{A}_{|j|}^{-n} \left(1 + \delta_{j0}\right) \mathcal{P}_{k-j-m}^{mW} e^{im\delta l} e^{ikl}. \end{aligned} \tag{2.23}$$

In this form, we can again recognize the Hansen coefficients as

$$X_k^{n,m} = \sum_{j=-\infty}^{\infty} \frac{1}{2} \mathcal{A}_{|j|}^{-n} \left(1 + \delta_{j0}\right) \mathcal{P}_{k-j-m}^{mW} e^{im\delta l}, \tag{2.24}$$

which are not constant anymore, but instead are slowly varying over time because of the dependence on δl. As soon as one goes to post-Newtonian orders, the Hansen coefficients are not functions of the eccentricity alone anymore. First there are three eccentricities appearing, but they can be expressed by each other (see Ref. [16] for explicit relations), such that we can work with only one of them. Here we choose the time eccentricity e_t. Second the symmetric mass ratio η appears, which is defined as

$$\eta = \frac{m_1 m_2}{(m_1+m_2)^2}. \tag{2.25}$$

For equal mass binaries its value is $\eta = 0.25$. Third the post-Newtonian parameter x occurs and indicates the corresponding PN order. We provide again the two coefficients $X_2^{-2,2}$ and $X_{-1}^{-3,4}$, expanded in eccentricity to $\mathcal{O}(e_t^{12})$, but now at first post-Newtonian order:

$$\begin{aligned} X_2^{-2,2} = \Bigg[& 1 - \frac{7}{2}e_t^2 + \frac{29}{16}e_t^4 - \frac{53}{288}e_t^6 + \frac{19}{288}e_t^8 + \frac{923}{28800}e_t^{10} + \frac{207871}{8294400}e_t^{12} \\ & + x\left(e_t^2(-32+\eta) + e_t^4\left(\frac{69}{8}+\eta\right) + e_t^6\left(\frac{85}{16}-\frac{13}{48}\eta\right) + e_t^8\left(\frac{34339}{4608}-\frac{37}{576}\eta\right) \right. \\ & \left. + e_t^{10}\left(\frac{687487}{76800}-\frac{691}{5760}\eta\right) + e_t^{12}\left(\frac{18765571}{1843200}-\frac{94033}{691200}\eta\right) \right) \Bigg] e^{2i\delta l}, \end{aligned} \tag{2.26a}$$

$$\begin{aligned} X_{-1}^{-3,4} = \Bigg[& \frac{11}{3840}e_t^5 + \frac{407}{92160}e_t^7 + \frac{4979}{1032192}e_t^9 + \frac{333757}{70778880}e_t^{11} \\ & + x\left(e_t^5\left(-\frac{29}{320}+\frac{1}{512}\eta\right) - e_t^7\left(\frac{217}{720}+\frac{821}{184320}\eta\right) \right. \\ & \left. - e_t^9\left(\frac{268531}{430080}+\frac{15621}{1146880}\eta\right) - e_t^{11}\left(\frac{1342661}{1290240}+\frac{7328539}{330301440}\eta\right) \right) \Bigg] e^{4i\delta l}. \end{aligned} \tag{2.26b}$$

Note that we do not expand the periastron precession term, since we do not want to mix terms varying on the different timescales.

2.3 Waveform

2.3.1 Newtonian waveform

We are now in the position to write the waveform polarization states using the Hansen coefficients. In quadrupolar, Newtonian order the time-domain amplitudes for the two polarizations $h_{+,\times}$ from an eccentric binary inspiral are adapted from Eq. (23) of Ref. [14] and listed here:

$$\begin{aligned} h_+^{\mathrm{N}} = \frac{G\,M\,\eta}{2R\,c^2}\frac{x}{(1-e_t\cos u)^2}\Bigg\{ & \sin^2\Theta\left(-e_t^2 + 2e_t\cos u - e_t^2\cos(2u)\right) - (1+\cos^2\Theta) \\ & \times\left[\left(4-3e_t^2-2e_t\cos u+e_t^2\cos(2u)\right)\cos(2(\phi-\Phi)) + 4\sin u\, e_t(1-e_t^2)^{1/2}\sin(2(\phi-\Phi))\right]\Bigg\}, \end{aligned} \tag{2.27a}$$

$$\begin{aligned} h_\times^{\mathrm{N}} = \frac{G\,M\,\eta}{R\,c^2}\frac{x\,\cos\Theta}{(1-e_t\cos u)^2}\Bigg\{ & 4\sin u\, e_t(1-e_t^2)^{1/2}\cos(2(\phi-\Phi)) \\ & - \left(4-3e_t^2-2e_t\cos u+e_t^2\cos(2u)\right)\sin(2(\phi-\Phi))\Bigg\}. \end{aligned} \tag{2.27b}$$

In these equations we have employed the convention defined in Section 1.2.5. So the source direction is specified by (Θ, Φ) and R is the distance from the source to the observer.

As we can see, the waveforms consist of terms $(1 - e_t \cos u)^{-2}$ times a trigonometric function of ϕ. We therefore can invoke the series expansion involving the Hansen coefficients. To increase readability, we set the constant angle $\Phi = 0$. For arbitrary Φ one would have to multiply each Hansen coefficient $X_j^{n,m}$ by $e^{-im\Phi}$. Furthermore, there are trigonometric functions of u appearing in the waveforms. For those we insert the series expansion in harmonics of l explicitly given in Eq. (A.4). This procedure allows us to write the waveform polarizations compactly as a sum over harmonics in l,

$$h_+ = \frac{G\,M\,\eta\,x}{c^2\,R} \sum_{s=-\infty}^{\infty} Q_s^+\, e^{isl}, \tag{2.28a}$$

$$h_\times = \frac{G\,M\,\eta\,x}{c^2\,R} \sum_{s=-\infty}^{\infty} Q_s^\times\, e^{isl}, \tag{2.28b}$$

where the $Q_s^{+,\times}$ are a sum over coefficients ϵ_j^{nu} and the Hansen coefficients $X_j^{n,m}$ and explicitly read

$$\begin{aligned} Q_s^+ = \sum_{j=-\infty}^{\infty} \frac{1}{2}\Bigg\{ & \sin^2\Theta\, e_t \left(\epsilon_j^{-1u} + \epsilon_j^{1u}\right) X_{s-j}^{-1,0} - (1+\cos^2\Theta) \\ & \times \Bigg[\left(\left(2 - \frac{3}{2}e_t^2\right)\delta_{s-j,0} + \frac{e_t}{2}\left(\frac{e_t}{2}\epsilon_{s-j}^{-2u} + \frac{e_t}{2}\epsilon_{s-j}^{2u} - \epsilon_{s-j}^{-1u} - \epsilon_{s-j}^{1u}\right)\right) \\ & \times \left(X_j^{-2,-2} + X_j^{-2,2}\right) - e_t\sqrt{1-e_t^2}\left(\epsilon_{s-j}^{-1u} - \epsilon_{s-j}^{1u}\right)\left(X_j^{-2,-2} - X_j^{-2,2}\right)\Bigg]\Bigg\}, \end{aligned} \tag{2.28c}$$

$$\begin{aligned} Q_s^\times = \sum_{j=-\infty}^{\infty} i\,\cos\Theta\Bigg\{ & \left(\left(2 - \frac{3}{2}e_t^2\right)\delta_{s-j,0} + \frac{e_t}{2}\left(\frac{e_t}{2}\epsilon_{s-j}^{-2u} + \frac{e_t}{2}\epsilon_{s-j}^{2u} - \epsilon_{s-j}^{-1u} - \epsilon_{s-j}^{1u}\right)\right) \\ & \times \left(X_j^{-2,-2} - X_j^{-2,2}\right) - e_t\sqrt{1-e_t^2}\left(\epsilon_{s-j}^{-1u} - \epsilon_{s-j}^{1u}\right)\left(X_j^{-2,-2} + X_j^{-2,2}\right)\Bigg\}. \end{aligned} \tag{2.28d}$$

For instance, the coefficient Q_1^+ expanded to $\mathcal{O}(e_t^8)$ is

$$Q_1^+ = \sin^2\Theta\left(\frac{e_t}{2} - \frac{e_t^3}{16} + \frac{e_t^5}{384} - \frac{e_t^7}{18432}\right) + (1+\cos^2\Theta)\left(\frac{3e_t}{4} - \frac{e_t^3}{3} + \frac{37e_t^5}{1536} - \frac{11e_t^7}{15360}\right), \tag{2.29}$$

and can be compared to Eq. (47a) in Ref. [14]. Be aware that their $h_{+,\times}$ is defined with an additional minus sign (Eq. (46)) and they use a trigonometric form instead of an exponential form, which causes an overall factor of 2.

Note that it is possible to write the Newtonian order waveform with a sum just over the Hansen coefficients, instead of the two sums in Eqs. (2.28a) and (2.28b). This is because it can be rewritten in terms of the true anomaly v instead of the eccentric anomaly u. For example taking the h_+ given in Eq. (48) of Ref. [14] in terms of v, we can directly insert the Hansen coefficients and write

$$\begin{aligned} h_+ = -\frac{G\,M\,\eta}{c^2\,R}\frac{x}{1-e^2} \sum_{s=-\infty}^{\infty} \Big\{ & (1+\cos^2\Theta)\Big(\left(X_s^{0,-2} + X_s^{0,2}\right) + \frac{5e}{4}\left(X_s^{0,-1} + X_s^{0,1}\right) \\ & + \frac{e}{4}\left(X_s^{0,-3} + X_s^{0,3}\right) + e^2 X_s^{0,0}\Big) + \sin^2\Theta\left(\frac{e}{2}\left(X_s^{0,-1} + X_s^{0,1}\right) + e^2 X_s^{0,0}\right)\Big\}\, e^{isl}. \end{aligned} \tag{2.30}$$

However, it is difficult to extend this form to post-Newtonian orders, because in doing so the angle ϕ is not anymore given directly by the true anomaly, but instead the periastron advance and higher order terms appear.

2.3.2 Post-Newtonian waveform

Post-Newtonian waveform polarizations can generally be written in the form

$$h_{+,\times} = \frac{G\,M\,\eta\,x}{c^2\,R} H_{+,\times}, \tag{2.31a}$$

$$H_{+,\times} = \sum_{n=0}^{\infty} x^{n/2} H_{+,\times}^{(n/2)}, \tag{2.31b}$$

where the power of x indicates the PN-order. The $H_{+,\times}^{(n/2)}$ are then given as the series expansions in terms of the mean anomaly l at the respective order. At Newtonian order we have

$$H_{+,\times}^{(0)} = \sum_{s=-\infty}^{\infty} Q_s^{+,\times\,(0)}\, e^{isl}, \tag{2.32}$$

where the $Q_s^{+,\times\,(0)}$ (the zero indicates the PN order) have been derived above in Eqs. (2.28c) and (2.28d). The next higher order terms, $Q_s^{+,\times\,(1/2)}$ and $Q_s^{+,\times\,(1)}$, are provided in Appendix B, since the expressions tend to get lengthy.

Notice that the $Q_s^{+,\times}$ at Newtonian order are constants, but because they are given in terms of the Hansen coefficients, they begin to vary slowly on the periastron precession timescale due to the factor $e^{im\delta l}$ as soon as one invokes PN corrections.

2.3.3 Radiation-reaction

Since a binary system has a time varying mass quadrupole, according to the quadrupole formula (Eq. (1.39)) it radiates energy in gravitational waves. This energy is drained from the binaries orbital energy and angular momentum, which therefore affect the binaries eccentricity and its semi-major axis. Due to Kepler's laws, a change in the semi-major axis also affects the frequency. The equations that govern this process are at leading order given by [25]:

$$\frac{de_t}{dt} = -\frac{(G\,M\,n)^{5/3}\,n\,\eta\,e_t}{15\,c^5\,(1-e_t^2)^{5/2}}\big[304 + 121\,{e_t}^2\big], \tag{2.33a}$$

$$\frac{dn}{dt} = \frac{(G\,M)^{5/3}\,n^{11/3}\,\eta}{5\,c^5\,(1-e_t^2)^{7/2}}\big[96 + 292\,{e_t}^2 + 37\,{e_t}^4\big]. \tag{2.33b}$$

They influence the binaries motion at $\mathcal{O}(c^{-5})$ order and are therefore 2.5PN corrections. Looking at the equations one observes that the eccentricity decreases with time, so the orbit becomes more and more circular and the orbital frequency n increases.

2.3.4 Fourier transform of the waveform

For the purpose of data analysis of gravitational wave signals measured in detectors, a waveform model in the frequency domain is desired. The waveforms given above depend on the mean anomaly l which is directly related to time. To calculate this Fourier transform analytically is not possible due to the complexity of the time-domain waveform. One could transform the time-domain waveforms numerically, but this is computationally intensive because the waveform needs to be sampled at a rate given by the orbital period. Luckily, there is an approximation called the stationary phase approximation (SPA), which is useful in calculating the Fourier transform of a function evolving on different time scales. We sketch this approach following Ref. [26].

Remembering the formula for the waveform polarizations given in Eqs. (2.28a) and (2.28b), it can be described in the following form

$$h(t) = A(t)e^{-i\Phi(t)}, \tag{2.34}$$

where $h(t)$ oscillates on the orbital timescale and its amplitude $A(t)$ and frequency evolve on the slower periastron-advance and radiation-reaction time scales. The Fourier transform of Eq. (2.34) is given by

$$\tilde{h}(f) = \int dt\, A(t)e^{-i\Phi(t)}e^{2\pi i f t} = \int dt\, A(t)e^{i\phi(f,t)}. \tag{2.35}$$

At a given frequency f, the Fourier integral is dominated by the contributions where the phase is slowly varying. In the regions where the integrand oscillates rapidly, the contributions are small. This allows us to define the stationary phase points as the times $t_{\rm SPA}$ where the derivative of the phase is zero ($\dot{\phi}(f, t_{\rm SPA}) = 0$), which is equivalent to

$$\dot{\Phi}(t_{\rm SPA}) = 2\pi f. \tag{2.36}$$

At this point the phase can be Taylor expanded and therefore it is possible to calculate the Fourier integral analytically. The waveform in the Fourier domain then reads

$$\tilde{h}_{\rm SPA}(f) = \left[\frac{2}{|\ddot{\Phi}(t_{\rm SPA})|}\right]^{1/2} A(t_{\rm SPA})\Gamma\Big(\frac{1}{2}\Big)e^{i[2\pi f t_{\rm SPA} - \Phi(t_{\rm SPA}) - \sigma\pi/4]}, \tag{2.37}$$

where $\sigma = \text{sign}(\ddot{\Phi}(t_{\rm SPA}))$, $\Gamma(.)$ is the Gamma function and $t_{\rm SPA}$ is understood as a function of frequency. Several assumptions need to be satisfied to justify the use of the SPA, which have been taken for granted here. For example the second derivative of $\Phi(t_{\rm SPA})$ may not vanish, so that it is sufficient to expand to second order, or that there is a unique stationary phase point.

From this general approach we now move on to the Fourier transform of the waveforms given in Eqs. (2.28a) and (2.28b). For the sake of convenience we specialize to the Newtonian order waveforms. The Fourier transform of the waveform polarizations becomes

$$\tilde{h}_{+,\times}(f) = \frac{(G\,M)^{5/3}\eta}{c^4 R}\int dt \sum_{s=-\infty}^{\infty} n(t)^{2/3}\, Q_s^{+,\times}(t)\, e^{i(snt+2\pi f t)}, \tag{2.38}$$

where we have inserted $x = \big(\frac{GMn}{c^3}\big)^{2/3}$. By introducing the effects of radiation-reaction, the orbital frequency n and the Q_s^+, which are depending on the eccentricity, become functions of time. Expressions for $n(t)$ and $e_t(t)$ can be found by solving the system of differential equations given in Section 2.3.3. The mean anomaly is related to time by the definition $\dot{l} = n$ and therefore

$$l(t) = \int_{t_0}^{t} dt'\, n(t'). \tag{2.39}$$

The condition for the stationary phase points given in Eq. (2.36) leads to

$$sn(t) + 2\pi f = 0. \tag{2.40}$$

Solving numerically for t gives the time $t_{\rm SPA}$ as a function of f. Having found $t_{\rm SPA}$, we use Eq. (2.37) to write the Fourier transformed waveform in the stationary phase approximation as

$$\tilde{h}_{\rm SPA_+}(f) = \frac{(G\,M)^{5/3}\eta}{c^4 R}\sum_{s=-\infty}^{\infty}\left[\frac{2}{|s\dot{n}(t_{\rm SPA})|}\right]^{1/2} n(t_{\rm SPA})^{2/3} Q_s^+(t_{\rm SPA})\Gamma\Big(\frac{1}{2}\Big)e^{i[2\pi f t_{\rm SPA} + sl(t_{\rm SPA}) - \sigma\pi/4]}. \tag{2.41}$$

In Fig. 2.1 we took a piece of a waveform in time-domain and Fourier transformed it once using the stationary phase approximation and once evaluating the Fourier integral in Eq. (2.38)

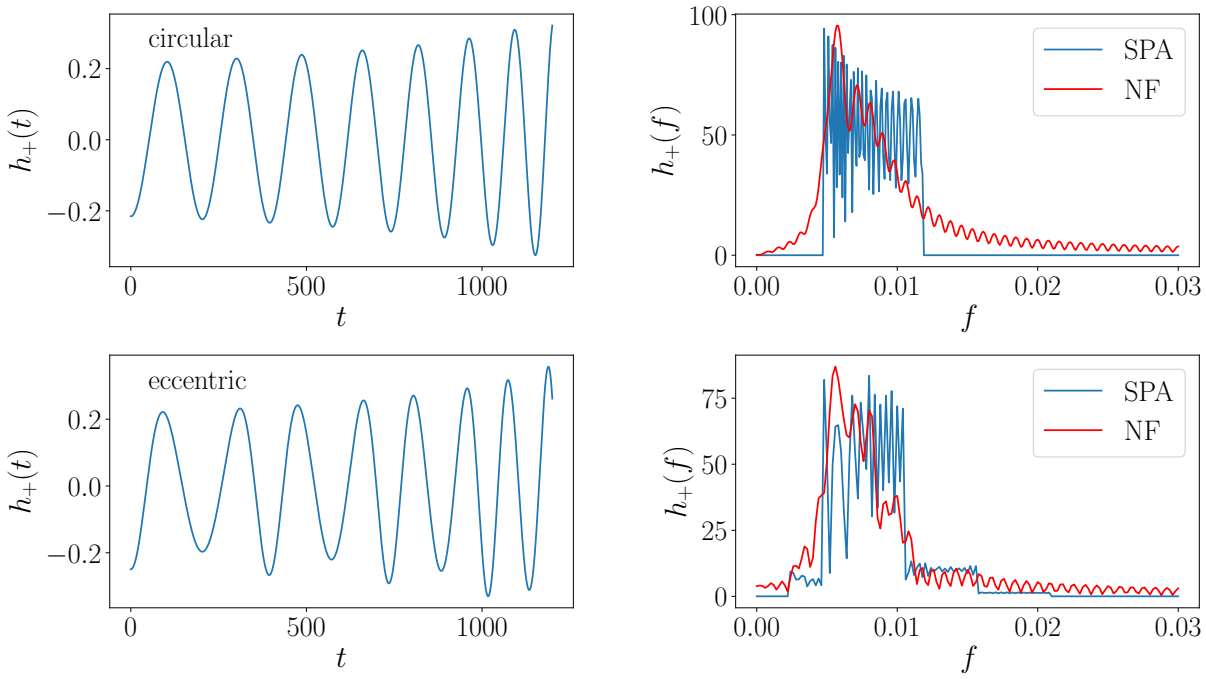

Figure 2.1: Fourier transform of a piece of the waveform polarization h_+. The h_+ in the time-domain is shown on the left-hand side, at the top in the circular limit and at the bottom with a low eccentricity. On the right-hand side the Fourier transformed waveforms are displayed, using two different methods. Once they are obtained using the stationary phase approximation (SPA) and the other by computing the Fourier integral numerically (NF). The constants in front of Eqs. (2.38) and (2.41) have been removed, so we just had to set an initial frequency and eccentricity, ($n(0) = 0.015$, $e(0) = 0.0$) in the top row and ($n(0) = 0.015$, $e(0) = 0.1$) in the bottom, a symmetric mass ratio ($\eta = 0.25$) and an inclination angle $\Theta = 0.5$.

numerically. We just took the Newtonian expressions for the $h_+(t)$ but introduced radiation-reaction effects, which cause the frequency and amplitude of the $h_+(t)$ in time-domain to increase. Going full post-Newtonian tends to get difficult because of the periastron advance, which would modify the stationary phase condition in Eq. (2.40) and one would need to distinguish between different cases. A discussion can be found in Ref. [24].

In the circular limit, only one Q_s^+-mode is nonzero, the $s = \pm 2$, whereas in the eccentric case more modes contribute. This can also be recognized in Fig. 2.1, the Fourier transform of the circular waveform has just one frequency part where it is nonzero, whereas the eccentric one has several steps.

3 Gravitational wave memory from eccentric binaries

The purpose of this chapter is to explain the gravitational wave memory effect and calculate first post-Newtonian (PN) corrections to the memory from eccentric binary inspirals. We will start with a description of the memory effect and afterwards review the post-Newtonian wave generation formalism to find a formula for the memory. We will go on calculating the memory to 1PN order and explore its effect on the waveform. At last, we will shortly discuss the probability of detecting the memory effect with gravitational wave interferometers.

3.1 Introduction to the memory effect

Usually, one thinks of gravitational waves as purely oscillatory phenomena. For example, the coalescence of black holes and neutron stars that have been observed with the LIGO detector follow a characteristic structure. The amplitude and phase increase during the inspiral, peak when the merger happens and decay afterwards to zero during the ringdown. However, gravitational waves have a property called gravitational memory, which manifests in a difference of the observed gravitational wave polarization amplitudes at late and early times

$$\Delta h_{+,\times} = \lim_{t\to\infty} h_{+,\times} - \lim_{t\to-\infty} h_{+,\times}. \tag{3.1}$$

In an ideal gravitational wave detector, one that is freely falling, the memory causes a permanent displacement after the gravitational wave has passed. Two types of memory exist, linear and non-linear. We will shortly discuss both before concentrating on the non-linear memory, which is predominant in bound binary systems.

3.1.1 Linear memory effect

The linear memory was first described in 1974 [27] and originates mainly from non-oscillatory motions of the source, more precisely from a net change in the time derivatives of the source-multipole moments. An example would be a binary on a hyperbolic orbit or in general systems that change from a bound state to being unbound. This includes supernova explosions and associated Neutron star kicks [28, 29, 30], gamma-ray burst jets [31, 32] and asymmetric mass loss due to neutrino emission [28, 33, 34, 35]. Thorne [36] provided a general formula for the linear memory produced by a system of N bodies,

$$\Delta h_{jk}^{\mathrm{TT}} = \Delta \sum_{A=1}^{N} \frac{4M_A}{R\sqrt{1-v_A^2}} \left[\frac{v_A^j v_A^k}{1-\vec{v}_A\cdot\vec{N}}\right]^{\mathrm{TT}}, \tag{3.2}$$

where the masses are unbound in their initial and/or final state. The Δ signifies to take the difference between final and initial values of the summation over the changing masses M_A or velocities $\vec{v}_A$. $\vec{N}$ is a unit vector that points from the source to the observer. This formula is the standard Liénard-Wiechert solution to the space-space part of the linearized Einstein equations,

with a stress-energy tensor given by N non-interacting particles. The masses and velocities could stand for pieces of a disrupting star, individual neutrinos becoming unbound or bodies on a gravitational scattering orbit.

3.1.2 Non-linear memory effect

The non-linear memory is a phenomenon directly related to the non-linearity of general relativity. Loosely speaking it is due to gravitational waves emitted by gravitational waves. More technically, the radiative-multipole moments are changed because of the energy flux from the radiated gravitational waves. The non-linear memory is often referred to as the "Christodoulou memory", after one of its discoverers. In fact, it was discovered independently by Christodoulou [37], Blanchet and Damour [38], and Payne [39].

The origin of the non-linear memory can be understood directly from the Einstein field equations

$$R^{\mu\nu} - \frac{1}{2} g^{\mu\nu} R = 8\pi T^{\mu\nu}, \tag{3.3}$$

where $R^{\mu\nu}$ is the Ricci tensor, $g^{\mu\nu}$ is the spacetime metric and $T^{\mu\nu}$ is the stress energy tensor. For practical calculations involving gravitational waves it is conventional to define the potential

$$h^{\mu\nu} = \eta^{\mu\nu} - \sqrt{-g}\, g^{\mu\nu}, \tag{3.4}$$

where $\eta^{\mu\nu}$ is the flat spacetime metric and g is the determinant of the metric. Note that we have not performed a weak field expansion, so we are working in full general relativity. The spatial components of $h^{\mu\nu}$ far away from the source are directly related to the signal a gravitational wave detector measures. By the condition

$$h^{\mu\nu}{}_{,\nu} = 0 \tag{3.5}$$

one specifies to a particular gauge, the de Donder or harmonic gauge. The Einstein equations then take the form

$$\Box h^{\mu\nu} = -16\pi \tau^{\mu\nu}, \tag{3.6}$$

where $\Box = -\partial_t^2 + \nabla^2$ is the flat spacetime d'Alembert operator and on the right-hand side is an effective stress-energy pseudotensor,

$$\tau^{\mu\nu} = (-g)(T^{\mu\nu} + t^{\mu\nu}_{\rm LL}) + \frac{1}{16\pi} \left(h^{\mu\rho}{}_{,\sigma}\, h^{\nu\sigma}{}_{,\rho} - h^{\rho\sigma} h^{\mu\nu}{}_{,\rho\sigma} \right), \tag{3.7}$$

involving the Landau-Lifshitz pseudotensor $t^{\mu\nu}_{\rm LL}$ (see e.g. Eq. (2.7) in Ref. [40]) which loosely speaking stands for the gravitational field energy. Note that the last term of Eq. (3.7) involves a second derivative and therefore actually modifies the wave operator on the left hand side of Eq. (3.6). This is another interesting non-linear effect, it can be physically interpreted as the backscattering of gravitational radiation as it propagates through curved spacetime. This term leads to so called tail effects [41].

In order to understand the non-linear memory effect, we focus on another piece of $t^{\mu\nu}_{\rm LL}$ that is equal to the gravitational wave stress-energy tensor (Eq. (1.31)) [42],

$$t_{jk} = \frac{1}{32\pi} \left\langle h^{\rm TT}_{ab,j}\, h^{\rm TT}_{ab,k} \right\rangle \approx t_{00} n_j n_k = \frac{1}{R^2} \frac{dE^{\rm GW}}{dt\, d\Omega} n_j n_k, \tag{3.8}$$

where $\frac{dE^{\rm GW}}{dt\, d\Omega}$ is the gravitational wave energy flux and n_j is a unit radial vector. The approximate sign means to take the plane-wave approximation $h^{\rm TT}_{ab} \approx F_{ab}(t-R)/R + \mathcal{O}(1/R^2)$ and the angle brackets imply to average over several wavelengths.

To get the solution of the wave equation (Eq. (3.6)), one applies Green's function to the source term on the right-hand side. The term involving the gravitational wave stress-energy tensor causes the following correction to the gravitational wave potentials

$$\delta h_{jk}^{\rm TT} = \frac{4}{R}\int_{-\infty}^{T_R} dt' \left[\int \frac{dE^{\rm GW}}{dt'\, d\Omega'} \frac{n'_j n'_k}{(1-\vec{n}'\cdot\vec{N})} d\Omega'\right]^{\rm TT}, \tag{3.9}$$

where T_R is the retarded time. The time-integral is quite interesting, the memory piece at any point of retarded time depends on the entire past history of the source system. This is what gives the memory its hereditary nature. If the unbound objects are assumed to be the individual gravitons with energies $E_A = M_A/(1-v_A^2)^{1/2}$ and velocities $v_A^j = cn_A^j$, the non-linear memory can be described with the same formula as the linear memory (Eq. (3.2)) [36].

As mentioned above, the non-linear memory can be physically interpreted as the part of the gravitational field in the radiation zone, that is sourced by the loss of gravitational wave energy in a system.

3.2 Post-Newtonian wave generation formalism

3.2.1 Gravitational wave multipole decomposition

In the radiation-zone, the most general outgoing-wave solution of the vacuum wave equation $\Box h_{ij}^{\rm TT} = 0$ can be written as a decomposition in radiative mass- and current-multipole moments [13]:

$$h_{ij}^{\rm TT} = \frac{4G}{Rc^2}\Lambda_{ijkl}\sum_{l=2}^{\infty}\frac{1}{c^l l!}\left[\mathcal{U}_{klL-2}(T_R)N_{L-2} + \frac{2l}{c(l+1)}\epsilon_{pq(k}\,\mathcal{V}_{l)pL-2}(T_R)N_{qL-2}\right] + \mathcal{O}\left(\frac{1}{R^2}\right). \tag{3.10}$$

Here the radiative mass- and current-multipole moments $\mathcal{U}_L(T_R)$ and $\mathcal{V}_L(T_R)$ are symmetric trace-free (STF) tensors which have l indices $i_1 i_2 ... i_l$ and have to be evaluated at retarded time $T_R = T - R$. The Λ_{ijkl} is the projection operator to the transverse-traceless gauge defined in Eq. (1.16).

Instead of using the decomposition into STF radiative multipoles $\mathcal{U}_L$ and $\mathcal{V}_L$, for the purpose of calculating the memory, it is beneficial to work with a mode decomposition of the combination $h_+ - ih_\times$ into scalar multipole moments

$$h_+ - ih_\times = \sum_{l=2}^{\infty}\sum_{m=-l}^{l} h^{lm}\,{}_{-2}Y^{lm}(\Theta,\Phi), \tag{3.11}$$

where

$$h^{lm} = \frac{G}{\sqrt{2}Rc^{l+2}}\left[U^{lm}(T_R) - \frac{i}{c}V^{lm}(T_R)\right]. \tag{3.12}$$

The ${}_{-2}Y^{lm}(\Theta,\Phi)$ are called spin-weighted spherical harmonics or tensor spherical harmonics and are defined in terms of the Wigner d functions by

$${}_sY^{lm}(\Theta,\Phi) = (-1)^{-s}\sqrt{\frac{2l+1}{4\pi}}d^l_{m\,-s}(\Theta)e^{im\Phi}, \tag{3.13}$$

where

$$\begin{aligned} d^l_{ms}(\Theta) = {} & \sqrt{l(+m)!(l-m)!(l+s)!(l-s)!} \\ & \times \sum_{k=k_i}^{k_f}\frac{(-1)^k\left(\sin\frac{\Theta}{2}\right)^{2k+s-m}\left(\cos\frac{\Theta}{2}\right)^{2l+m-s-2k}}{k!(l+m-k)!(l-s-k)!(s-m+k)!}, \end{aligned} \tag{3.14}$$

and the sum goes from $k_i = \max(0, m-s)$ to $k_f = \min(l+m, l-s)$. The complex conjugates of the tensor spherical harmonics satisfy the identity

$$ {}_sY^{lm*} = (-1)^{s+m}\, {}_{-s}Y^{l-m}. \tag{3.15}$$

The complete relationships between the multipole decompositions in terms of STF tensors and "scalar" mass and current multipoles can be found in Ref. [43].

3.2.2 Relating radiative moments to source moments

The next step is to relate the radiative mass- and current-multipoles in the wave-zone to the source-multipole moments which are constructed from integrals over the stress-energy tensor of the source including its matter and gravitational fields. One method to relate these multipole moments is the multipolar-post-Minkowskian (MPM) formalism developed by Blanchet et al. We will shortly describe the main steps here, for a detailed review see Ref. [44].

The goal is to solve the Einstein field equation satisfying the harmonic gauge condition with a post-Minkowskian iteration. For this we expand the metric perturbation $h^{\mu\nu}$ in powers of the gravitational constant G,

$$ h^{\mu\nu} = G h_1^{\mu\nu} + G^2 h_2^{\mu\nu} + ... + G^n h_n^{\mu\nu} + ..., \tag{3.16}$$

and substitute it into the vacuum field equations. This leads to a system of wave equations, each satisfying the harmonic gauge condition $h_n^{\mu\nu}{}_{,\nu} = 0$,

$$ \Box h_n^{\mu\nu} = \Lambda_n^{\mu\nu}\left[h_1, ..., h_{n-1}\right], \tag{3.17}$$

where $\Lambda_n^{\mu\nu}$ represents the respective expansion of the right-hand side of Eq. (3.6) with $T^{\mu\nu} = 0$.

The $h_n^{\mu\nu}$ can then be expanded in L/r, $L < r$ being the size of the source and r the field point, and the coefficients of the powers of L/r interpreted as a new family of multipole moments. The most general solution for $h_1^{\mu\nu}$ valid outside the source can be written with two new STF moments, $\mathcal{M}_L$ and $\mathcal{S}_L$ [43]. They represent canonical mass- and current-multipole moments that have an intermediate function between radiative and source moments. Substituting the linear solution into the right-hand side of Eq. (3.17), the next order can be calculated and so on, resulting in a multipole expansion in terms of the canonical moments $h_n^{\mu\nu} = h_n^{\mu\nu}\left[\mathcal{M}_L, \mathcal{S}_L\right]$.

This expansion has to be regularized at $r = 0$ because the standard retarded Green's function operator would yield divergent integrals and one has to add an additional piece in order to satisfy the harmonic gauge condition. For details see Ref. [38]. The result for $h_n^{\mu\nu}$ has to be transformed from the harmonic coordinates describing the source to radiative coordinates introduced at the beginning of this section. After taking the TT piece of $h_n^{\mu\nu}$ one can compare with Eq. (3.10) and read off the relations between the radiative- and canonical-multipole moments. Complete results of this procedure can be found in Ref. [45], we will just state the result for the radiative mass quadrupole because it includes the non-linear memory term:

$$\begin{aligned}
\mathcal{U}_{ij}(T_R) = {} & \mathcal{M}_{ij}^{(2)}(T_R) + \frac{2G\mathcal{M}}{c^3}\int_{-\infty}^{T_R} d\tau \mathcal{M}_{ij}^{(4)}(\tau)\left[\ln\left(\frac{T_R-\tau}{\tau_0}\right) + \frac{11}{12}\right] \\
& - \frac{2}{7}\frac{G}{c^5}\int_{-\infty}^{T_R} d\tau \mathcal{M}_{a\langle i}^{(3)}(\tau)\mathcal{M}_{j\rangle a}^{(3)}(\tau) + \frac{G}{c^5}\Big[\frac{1}{7}\mathcal{M}_{a\langle i}^{(5)}\mathcal{M}_{j\rangle a} \\
& - \frac{5}{7}\mathcal{M}_{a\langle i}^{(4)}\mathcal{M}_{j\rangle a}^{(1)} - \frac{2}{7}\mathcal{M}_{a\langle i}^{(3)}\mathcal{M}_{j\rangle a}^{(2)} + \frac{1}{3}\epsilon_{ab\langle i}\mathcal{M}_{j\rangle a}^{(4)}\mathcal{S}_b\Big] \\
& + \frac{2G^2\mathcal{M}^2}{c^6}\int_{-\infty}^{T_R} d\tau\left[\ln^2\left(\frac{T_R-\tau}{2\tau_0}\right) + \frac{57}{70}\ln\left(\frac{T_R-\tau}{2\tau_0}\right) + \frac{124627}{44100}\right]\mathcal{M}_{ij}^{(5)}(\tau) + \mathcal{O}(\frac{1}{c^7}).
\end{aligned} \tag{3.18}$$

The first term in this equation is the leading-order instantaneous term, depending directly on the retarded configuration of the source. It is similar to the standard quadrupole term but contains higher order corrections when expressed in terms of the source moments. The next two terms are hereditary because of the integral over the entire past history of the source. The first one is the tail term and the second one the non-linear memory term, which we will focus on later. The other terms on the second and third line are non-linear instantaneous terms of $\mathcal{O}(G^2)$. The term in the last line yields tails-of-tails like contributions to the radiative mass multipole.

The canonical moments $\mathcal{M}_L$ and $\mathcal{S}_L$ itself are related to six types of source-multipole moments: $\{\mathcal{I}_L, \mathcal{J}_L, \mathcal{W}_L, \mathcal{X}_L, \mathcal{Y}_L, \mathcal{Z}_L\}$. The dominating ones are the mass- and current-source moments $\mathcal{I}_L$ and $\mathcal{J}_L$, the other four enter only as 2.5 PN corrections. Using the same MPM iteration, one can write the metric perturbation at each post-Minkowskian order as a function of the source moments $h_n^{\mu\nu}[\mathcal{I}_L, \mathcal{J}_L, ...]$. These can then be related to the canonical moment solution $h_n^{\mu\nu}[\mathcal{M}_L, \mathcal{S}_L]$ via a gauge transformation. From the relationship between the two metrics one can express the canonical moments in terms of the source moments

$$\mathcal{M}_L = \mathcal{I}_L + G\,\delta\mathcal{I}_L + \mathcal{O}(G^2), \tag{3.19a}$$

$$\mathcal{S}_L = \mathcal{J}_L + G\,\delta\mathcal{J}_L + \mathcal{O}(G^2), \tag{3.19b}$$

where the correction terms $\delta\mathcal{I}_L$ and $\delta\mathcal{J}_L$ modify the leading order mass- and current source multipole moments starting at 2.5 PN order and are given through the six source moments.

In the last step we need to match the MPM expansion of the metric in terms of the source moments in the wave-zone to a post-Newtonian solution of the Einstein equations describing the source. The two approximations are both valid outside but close to the source, therefore one obtains an explicit relationship between the source moments and the PN-expansion of the near-zone metric. By solving the equations of motion of the source, one can find expressions for the source moments in terms of the variables describing the source (see Ref. [44] for the details of this non-trivial calculation).

3.2.3 Memory contribution to the radiative mass-multipole

The leading post-Minkowskian order contributions to the radiative mass- and current-multipole moments for arbitrary l are given by [38]:

$$\mathcal{U}_L = \mathcal{M}_L^{(l)} + G\mathcal{U}_L^{(\text{tail})} + G\mathcal{U}_L^{(\text{mem})} + \mathcal{O}(G^2) + \mathcal{O}(G/c^5), \tag{3.20a}$$

$$\mathcal{V}_L = \mathcal{S}_L^{(l)} + G\mathcal{V}_L^{(\text{tail})} + \mathcal{O}(G^2) + \mathcal{O}(G/c^5). \tag{3.20b}$$

All $\mathcal{O}(G^2)$ terms, which include cubically non-linear interactions and tail-of-tails like terms, as well as $\mathcal{O}(G/c^5)$ terms, which are instantaneous products of canonical moments-like terms, are neglected. We will not examine the tail contributions here, but instead go straightforward to the discussion of the memory. It only contributes to the radiative mass moment at $\mathcal{O}(G)$ and is given by [38]:

$$\mathcal{U}_L^{(\text{mem})} = \frac{2c^{l-2}(2l+1)!!}{(l+1)(l+2)} \int_{-\infty}^{T_R} dt \int d\Omega \frac{dE^{\text{GW}}}{dt\,d\Omega} n_{\langle L\rangle}. \tag{3.21}$$

In this equation $\frac{dE^{\text{GW}}}{dt\,d\Omega}$ is the gravitational wave energy flux and n_i is a general unit vector that points from the source center to the spherical polar angles (θ, ϕ). These angles, over which the integral has to be taken over, may not be mistaken for the angles (Θ, Φ) appearing in the waveform polarizations. Although Eqs. (3.20a) and (3.21) could mislead to think that only the energy flux at first post-Minkowskian order contributes to the memory, it follows from other derivations [46, 37] that Eq. (3.21) is naturally extended to higher post-Minkowskian orders by using the gravitational wave energy flux to the highest known PN order.

One also has to be aware of that potentially arising linear memory from changes in the derivatives of the canonical mass- and current moments $\mathcal{M}_L^{(l)}$ and $\mathcal{S}_L^{(l)}$ is ignored. This is a clearly valid approximation for astrophysical binaries whose components were formed, captured or underwent mass changes long before they enter the gravitational wave driven regime. For binaries inspiralling on a quasicircular orbit, that remain bound in the infinite past, the linear memory vanishes completely.

Note that although the non-linear, hereditary memory contribution to the radiative-current multipoles vanishes, there is another type of DC (non-oscillatory) effect occurring from the 1.5PN correction to the radiative current-octupole moment [47]. This effect is non-linear and nonhereditary and modifies only the $\times$-polarization at 2.5PN order. A physical interpretation is lacking at the moment, however, due to its high PN order it is of much less observational significance [48].

To be able to calculate the hereditary memory contribution, we need the gravitational wave energy flux in terms of the metric perturbations. It is computed from the gravitational wave stress-energy tensor and given by [43]

$$\frac{dE^{\mathrm{GW}}}{dt\,d\Omega} = R^2 t_{00} = \frac{R^2}{32\pi}\langle \dot{h}_{ij}^{\mathrm{TT}} \dot{h}_{ij}^{\mathrm{TT}} \rangle = \frac{R^2}{16\pi}\langle \dot{h}_{+}^2 + \dot{h}_{\times}^2 \rangle, \tag{3.22}$$

where the angle brackets imply to average over several wavelengths. Since we want the energy flux in terms of the scalar multipole modes h_{lm}, we use the expansion portrayed in Eq. (3.11) and get

$$\frac{dE^{\mathrm{GW}}}{dt\,d\Omega} = \frac{R^2}{16\pi} \sum_{l'=2}^{\infty} \sum_{l''=2}^{\infty} \sum_{m'=-l'}^{l'} \sum_{m''=-l''}^{l''} \langle \dot{h}_{l'm'} \dot{h}^*_{l''m''} \rangle \, {}_{-2}Y^{l'm'}(\theta,\phi) \, {}_{-2}Y^{l''m''*}(\theta,\phi). \tag{3.23}$$

Also Eq. (3.21) has to be transformed to the scalar radiative mass multipole with the help of the relations [43]

$$U^{lm} = A_l \, \mathcal{U}_L \, \mathcal{Y}_L^{lm*}, \tag{3.24a}$$

$$A_L = \frac{16\pi}{(2l+1)!!}\sqrt{\frac{(l+1)(l+2)}{2l(l-1)}}, \tag{3.24b}$$

$$Y^{lm} = \mathcal{Y}_L^{lm} n_L = \mathcal{Y}_L^{lm} n_{\langle L \rangle}. \tag{3.24c}$$

The last equation relates the STF spherical harmonics $\mathcal{Y}_L^{lm}$ to the ordinary scalar spherical harmonics. Putting everything together yields a formula for the memory piece of the scalar radiative mass multipole

$$U_{lm}^{(\mathrm{mem})} = \frac{32\pi}{c^{2-l}}\sqrt{\frac{(l-2)!}{2(l+2)!}} \int_{-\infty}^{T_R} dt \int d\Omega \, \frac{dE^{\mathrm{GW}}}{dt\,d\Omega}(\Omega) \, Y^*_{lm}(\Omega) \tag{3.25}$$

where one can directly insert the expression for the gravitational wave energy flux given in Eq. (3.23). According to Eq. (3.12), the memory contribution to the U^{lm} modes directly enters the waveform multipole modes h^{lm}.

3.3 Memory contribution to derivatives of multipole modes at 1PN order

Our goal is to calculate post-Newtonian corrections to the gravitational wave memory from eccentric, inspiralling, compact binaries, which causes a non-oscillatory correction to the gravitational wave polarizations. Favata [1] has calculated the memory contribution to the gravitational wave

polarizations from eccentric binaries at the leading Newtonian order. In an earlier paper [48], post-Newtonian corrections for quasicircular binaries were calculated. Before describing all the details of our calculations, let's state the overall strategy.

Since there is no memory contribution to the current multipole moments, the memory piece of the spherical harmonic modes of the polarization waveform is given by Eq. (3.12)

$$h_{lm}^{(\mathrm{mem})} = \frac{1}{\sqrt{2}R} U_{lm}^{(\mathrm{mem})}. \tag{3.26}$$

Using Eq. (3.25) and inserting the expression for the gravitational wave energy flux (Eq. (3.23)) yields the following formula for the memory

$$\begin{aligned} h_{lm}^{(\mathrm{mem})} &= \frac{16\pi}{R}\sqrt{\frac{(l-2)!}{(l+2)!}}\int_{-\infty}^{T_R} dt \int d\Omega\, \frac{dE_{\mathrm{gw}}}{dt\, d\Omega}(\Omega) Y^*_{lm}(\Omega) \\ &= R\sqrt{\frac{(l-2)!}{(l+2)!}}\sum_{l'=2}^{\infty}\sum_{l''=2}^{\infty}\sum_{m'=-l'}^{l'}\sum_{m''=-l''}^{l''}(-1)^{m+m''} G^{2-20}_{l'l''lm'-m''-m}\int_{-\infty}^{T_R} dt \left\langle \dot{h}_{l'm'}\dot{h}^*_{l''m''}\right\rangle, \end{aligned} \tag{3.27}$$

where the quantity $G^{s_1s_2s_3}_{l_1l_2l_3m_1m_2m_3}$ is an angular integral over three tensor spherical harmonics,

$$G^{s_1s_2s_3}_{l_1l_2l_3m_1m_2m_3} = \int d\Omega\, {}_{s_1}Y^{l_1m_1}\, {}_{s_2}Y^{l_2m_2}\, {}_{s_3}Y^{l_3m_3}. \tag{3.28}$$

Eq. (3.27) is the main formula we need to compute the memory. We begin by giving a simplified expression for the angular integral. Then we will carry on by calculating the multipole modes describing an eccentric binary system and their derivatives. Note that on the right-hand side the multipole modes themselves appear, however, it is valid to insert the multipoles without memory because the non-linear memory contribution to the non-linear memory is negligible. After the averaging procedure caused by the angle brackets we will receive terms for the derivatives of the memory multipole modes $h_{lm}^{(\mathrm{mem})(1)}$. The last step is then to integrate over the entire past history of the binary system. Performing a low eccentricity expansion will give us explicit results for the memory pieces of the h_{lm} modes, which can be inserted into the waveform polarizations.

3.3.1 Angular integral over three tensor spherical harmonics

We first take a look at the angular integral $G^{s_1s_2s_3}_{l_1l_2l_3m_1m_2m_3}$ given in Eq. (3.28). It can be simplified following Appendix A of Ref. [48]. An expression for the tensor spherical harmonics in terms of the Wigner d functions is stated in Eqs. (3.13) and (3.14). The angular integral term over three tensor spherical harmonics turns out to be of the form

$$\begin{aligned} G^{s_1s_2s_3}_{l_1l_2l_3m_1m_2m_3} &= (-1)^{s_1+s_2+s_3}\frac{[(2l_1+1)(2l_2+1)(2l_3+1)]^{1/2}}{(4\pi)^{3/2}} \\ &\quad\times \int_0^{2\pi} d\Phi\, e^{i(m_1+m_2+m_3)\Phi}\int_0^{\pi} d\Theta\, \sin\Theta\, d^{l_1}_{m_1s_1} d^{l_2}_{m_2s_2} d^{l_3}_{m_3s_3}. \end{aligned} \tag{3.29}$$

The Φ-integral is quickly evaluated to be

$$\int_0^{2\pi} d\Phi\, e^{i(m_1+m_2+m_3)\Phi} = 2\pi\delta^{-m_1}_{m_2+m_3}. \tag{3.30}$$

The more involved Θ-integral can be rewritten to read

$$\int_0^{\pi} d\Theta\, \sin\Theta\, d^{l_1}_{m_1s_1} d^{l_2}_{m_2s_2} d^{l_3}_{m_3s_3} = 2\sum_{k_1,k_2,k_3} g_1(k_1) g_2(k_2) g_3(k_3)\int_0^{\pi} d\Theta \left(\sin\frac{\Theta}{2}\right)^{2a-1}\left(\cos\frac{\Theta}{2}\right)^{2b-1}, \tag{3.31}$$

where $g_j(k_j)$ is given in terms of the various coefficients by

$$g_j(k_j) = \frac{(-1)^{k_j}\left[(l_j+m_j)!(l_j-m_j)!(l_j+s_j)!(l_j-s_j)!\right]^{1/2}}{k_j!(l_j+m_j-k_j)!(l_j-s_j-k_j)!(s_j-m_j+k_j)!}, \tag{3.32}$$

and a and b are defined in terms of $p_j = 2k_j + s_j - m_j$,

$$a = 1 + \frac{p_1+p_2+p_3}{2}, \tag{3.33a}$$

$$b = 1 + l_1 + l_2 + l_3 - \frac{p_1+p_2+p_3}{2}. \tag{3.33b}$$

The remaining integral over Θ is found in integral tables [49] and can be expressed in terms of gamma functions as

$$\int_0^\pi d\Theta \left(\sin\frac{\Theta}{2}\right)^{2a-1}\left(\cos\frac{\Theta}{2}\right)^{2b-1} = \frac{\Gamma(a)\Gamma(b)}{\Gamma(a+b)}. \tag{3.34}$$

Using these simplifications, a computer algebra program like *Mathematica* [50] can evaluate the angular integrals over three spin-weighted spherical harmonics quite fast.

3.3.2 1PN-accurate multipole derivatives $\dot{h}_{lm}$ for eccentric binary systems

We want to begin with the calculation of 1PN-accurate expressions for the gravitational wave multipole modes h_{lm} from inspiralling binaries in elliptical orbits. The corresponding instantaneous gravitational waveform polarizations h_+ and $h_\times$ are known to 3PN-accuracy [51]. By inverting the multipole expansion of the polarizations Eq. (3.11) with the help of the orthogonality relation for tensor spherical harmonics, we can find explicit expressions for the h_{lm} by evaluating the integral

$$h_{lm} = \int d\Omega\ (h_+ - ih_\times)_{-2}Y^*_{lm}(\Theta,\Phi). \tag{3.35}$$

1PN expressions for the waveform polarizations can be found in Appendix F of Ref. [14]. The orbital motion of the binary system is parametrized in terms of the eccentric anomaly u. As an example we provide the h_{20} mode to 1PN order:

$$\begin{aligned} h_{20} = 4\sqrt{\frac{2\pi}{15}}\frac{M\,\eta\,e_t\,x}{R(1-e_t\cos u)}\Big[&\cos u + \frac{x}{168(1-e_t^2)(1-e_t\cos u)^2}\Big(732e_t - 396e_t^3 \\ &+ 44e_t\eta - 44e_t^3\eta + \big(-732 + 315e_t^2 - 171e_t^4 - 44\eta - 7e_t^2\eta + 51e_t^4\eta\big)\cos u \\ &+ \big(108e_t + 228e_t^3 + 68e_t\eta - 68e_t^3\eta\big)\cos 2u + \big(-27e_t^2 - 57e_t^4 - 17e_t^2\eta + 17e_t^4\eta\big)\cos 3u\Big)\Big]. \end{aligned} \tag{3.36}$$

Note that h_{lm} modes with $m \neq 0$ have a factor proportional to $e^{-im\phi}$ where ϕ is the orbital phase. The multipole modes are calculated up to $l = 4$. All higher modes vanish at 1PN order.

To compute the time derivative of the multipole modes, we consider only the orbital phase ϕ and the eccentric anomaly u as a function of time and neglect the time evolution of eccentricity and x because these effects do not enter until 2.5PN order and are on a different, much longer timescale. Using the generalized quasi-Keplerian parametrization we can write ϕ in terms of u via the true anomaly v. At first post-Newtonian order we have

$$\phi = (1+k)v, \tag{3.37}$$

where k comes from the advance of the periastron and can be expressed in terms of the eccentricity and the PN parameter x,

$$k = \frac{3x}{1-e_t^2}. \tag{3.38}$$

At the moment, we do not insert this expression because we do not want to mix the orbital and periastron advance timescales when expanding in x and just let the $m \neq 0$ terms as $e^{-im(1+k)v}$.

The true anomaly and the eccentric anomaly are linked via Eq. (2.5c). We need its time derivative, which is

$$\dot{v} = \frac{\sqrt{1-e_\phi^2}}{1-e_\phi \cos u}\dot{u}, \tag{3.39}$$

and $\dot{u}$ can be computed via the Kepler equation (Eq. (2.2)) such that

$$\dot{u} = \frac{n}{1-e_t \cos u}. \tag{3.40}$$

Note that in Eq. (3.39) some angular eccentricity e_ϕ appears, but it can be expressed through e_t and reads at 1PN-order

$$e_\phi = e_t(1 + x(4-\eta)). \tag{3.41}$$

Since we want the multipole modes in terms of the post-Newtonian parameter x, we have to write n in terms of x with the help of Eq. (A1) in Ref. [52]

$$n = \frac{x^{3/2}}{M}\left[1 + \frac{x}{(1-e_t^2)^3}\left(-3 + 6e_t^2 - 3e_t^4\right)\right], \tag{3.42}$$

where only next-to-leading order terms are considered.

3.3.3 Time derivatives of the memory pieces to 1PN order ($m = 0$)

We first make the definition $d/dT_R\, h_{lm}^{(\mathrm{mem})} = h_{lm}^{(\mathrm{mem})(1)}$ that stands for the memory mode before doing the hereditary time integral. As one can see in Eq. (3.27), we essentially need to calculate a big sum consisting of products of $\dot{h}_{l'm'}\dot{h}^*_{l''m''}$ and the angular integral $G^{2-20}_{l'l''lm'-m''m}$. When specializing to the $m = 0$ memory contributions, because of the Kronecker delta function coming from the Φ-integral, only combinations with $m' = m''$ contribute to $h_{l0}^{(\mathrm{mem})(1)}$, whereas all other combinations are zero. Since every time one multiplies the $\dot{h}_{l'm'}$ with a complex conjugate with the same m', all exponential terms vanish and thus, there is no dependence on the orbital phase ϕ anymore.

Although the exponential terms are gone, the time derivatives caused factors $\sim (1+k)$, where we now can insert the expression for k given in Eq. (3.38) and expand the $\dot{h}_{l'm'}\dot{h}^*_{l''m''}$ terms in x. The leading order is x^5, so we truncate terms of $\mathcal{O}(x^7)$.

The next step is to do the averaging procedure which originates from the construction of a well-defined gravitational wave stress-energy tensor. For bound, eccentric orbits, the average over several wavelengths is done by averaging over one orbital period

$$\langle F(t)\rangle = \frac{1}{P_{\mathrm{orb}}}\int_0^{P_{\mathrm{orb}}} dt\, F(t), \tag{3.43}$$

where $P_{\mathrm{orb}} = 2\pi M/x^{3/2}$. Since we have parametrized the orbital motion with the eccentric anomaly u, we have to substitute it into the integral, yielding

$$\langle F(t)\rangle = \frac{x^{3/2}}{2\pi M}\int_0^{2\pi} du\, F(u)\frac{(1-e_t\cos u)M}{x^{3/2}}. \tag{3.44}$$

Evaluating this integral, we find the time derivative of the memory contribution to the multipole modes $h_{lm}^{(\mathrm{mem})}$. For the dominant $h_{20}^{(\mathrm{mem})(1)}$ memory mode we find

$$\begin{aligned} h_{20}^{(\mathrm{mem})(1)} &= \sqrt{\frac{2\pi}{15}}\frac{x^5\,\eta^2}{R\,(1-e_t^2)^{7/2}}\left[\frac{128}{7}+\frac{1160}{21}e_t^2+\frac{146}{21}e_t^4\right] \\ &\quad -\sqrt{\frac{\pi}{30}}\frac{x^6\,\eta^2}{R\,(1-e_t^2)^{9/2}}\left[\frac{9752}{63}-\frac{32}{21}\eta+e_t^2\left(-436+\frac{19352}{63}\eta\right)\right. \\ &\quad \left.+e_t^4\left(-\frac{18103}{21}+\frac{7468}{21}\eta\right)+e_t^6\left(-\frac{241}{6}+\frac{1285}{63}\eta\right)\right]. \end{aligned} \tag{3.45}$$

The leading order x^5 term can be compared to Eq. (2.27a) in Ref. [1], one just has to change from the semilatus rectum p to x by the Newtonian relation

$$p=(1-e_t^2)\frac{M}{x}, \tag{3.46}$$

and indeed, the terms are found to be equal.

Another important check is to take the circular limit (set $e_t=0$) and compare with the leading order and 1PN part of Eq. (3.13a) in Ref. [48] with the help of Eq. (3.26) to relate $h_{l0}^{(\mathrm{mem})(1)}$ and $U_{l0}^{(\mathrm{mem})(1)}$. This circular limit is found to be

$$h_{20}^{(\mathrm{mem})(1)}=\frac{128\sqrt{2\pi/15}\,x^5\,\eta^2}{7R}-\frac{\sqrt{\pi/30}\,x^6\,\eta^2}{R}\left(\frac{9752}{63}-\frac{32}{21}\eta\right), \tag{3.47}$$

and coincides for the two approaches.

It is a remarkable fact that for non-precessing binaries the h_{lm} modes are entirely given by the mass multipoles when $l+m$ is even and by the current multipoles when $l+m$ is odd [53]. Since only the mass multipoles contain memory terms, there is no memory contribution to modes where $l+m$ is odd. Therefore the next contributing mode is $h_{40}^{(\mathrm{mem})(1)}$, which is calculated to be

$$\begin{aligned} h_{40}^{(\mathrm{mem})(1)} &= \sqrt{\frac{\pi}{10}}\frac{x^5\,\eta^2}{R\,(1-e_t^2)^{7/2}}\left[\frac{64}{315}+\frac{22}{35}e_t^2+\frac{17}{210}e_t^4\right] \\ &\quad +\sqrt{\frac{\pi}{10}}\frac{x^6\,\eta^2}{R\,(1-e_t^2)^{9/2}}\left[-\frac{10133}{3465}+\frac{20620}{2079}\eta+e_t^2\left(-\frac{3301}{198}+\frac{826288}{10395}\eta\right)\right. \\ &\quad \left.+e_t^4\left(-\frac{38809}{3080}+\frac{225818}{3465}\eta\right)+e_t^6\left(-\frac{227}{240}+\frac{55789}{13860}\eta\right)\right], \end{aligned} \tag{3.48}$$

and again the quasi-circular limit agrees with Eq. (3.13b) in Ref. [48] and the Newtonian limit with Eq. (2.27c) in Ref. [1].

The last non-zero memory mode is $h_{60}^{(\mathrm{mem})(1)}$, it has no Newtonian part anymore and reads

$$\begin{aligned} h_{60}^{(\mathrm{mem})(1)} &= \sqrt{\frac{\pi}{1365}}\frac{x^6\,\eta^2}{R\,(1-e_t^2)^{9/2}}\left[\left(-\frac{839}{1386}+\frac{86}{33}\eta\right)+e_t^2\left(-\frac{6007}{924}+\frac{274}{11}\eta\right)\right. \\ &\quad \left.+e_t^4\left(-\frac{3611}{924}+\frac{1079}{77}\eta\right)+e_t^6\left(-\frac{347}{672}+\frac{59}{33}\eta\right)\right]. \end{aligned} \tag{3.49}$$

In the circular limit, this memory mode coincides with the 1PN part of Eq. (3.13c) in Ref. [48], too.

3.3.4 Time derivatives of the memory pieces to 1PN order ($m \neq 0$)

We now turn to the memory modes where $m \neq 0$. All modes that have an odd $l+m$ are zero. This follows directly from the fact that these modes are entirely given by the current multipole which does not contribute to the memory.

The computation of the non-zero $m \neq 0$ memory modes is more involved. This is due to the fact that in the sum over the $\dot{h}_{l'm'}\dot{h}^*_{l''m''}$ terms, the exponential part is not canceling out anymore. The time derivatives of the $h_{l'm'}$ modes are proportional to $\dot{h}_{l'm'} \sim e^{-im'(1+k)v}$. Before we insert the 1PN expression for k (Eq. (3.38)), we split off the part proportional to $\sim e^{-im'kv}$ and take it out of the orbital average. In the remaining part we insert the 1PN expression for k, make a series expansion and cut off terms of $\mathcal{O}(x^4)$ in the individual modes.

In the next step, we have to write the $\sim e^{-im'v}$ part in the multipole modes as a function of the eccentric anomaly u. To do so we use the Euler identity $e^{ix} = \cos x + i \sin x$ to write this factor with trigonometric functions of v, where we can insert the 1PN valid expressions [54]

$$\cos v = \frac{\cos u - e_\phi}{1 - e_\phi \cos u}, \tag{3.50a}$$

$$\sin v = \frac{(1-e_\phi^2)^{1/2} \sin u}{1 - e_\phi \cos u}, \tag{3.50b}$$

with e_ϕ given by Eq. (3.41). Having done so, we are in the position to evaluate the four sums in Eq. (3.27) and expand again in x keeping terms up to x^6. This yields for the Newtonian and the post-Newtonian parts of even and odd l-modes a lot of terms of the form

$$h^{(\mathrm{mem})(1)}_{l_{\mathrm{even}}m} \sim \frac{1}{(1-e_t\cos u)^{8+|m|}} \left(f_n(e_t)\cos(n\,u) + g_n(e_t)\sin(n\,u)\right), \tag{3.51a}$$

$$h^{(\mathrm{mem})(1)}_{l_{\mathrm{odd}}m} \sim \frac{1}{(1-e_t\cos u)^{9+|m|}} \left(f_n(e_t)\cos(n\,u) + g_n(e_t)\sin(n\,u)\right), \tag{3.51b}$$

where $f_n(e_t)$ and $g_n(e_t)$ are functions of eccentricity and n is an integer up to 10. When applying the orbital average as defined in Eq. (3.44), all terms involving a sine vanish. The other terms provide a sensible result that is proportional to e_t^m. One must not forget to reinsert the exponential term from the periastron advance e^{-imkv}, that we have split off at the beginning. We now list all the $m \neq 0$ $h^{(\mathrm{mem})(1)}_{lm}$ modes up to first post-Newtonian order, note that only modes with an even $l+m$ are non-zero and we have defined the mass difference ratio $\Delta = (m_1 - m_2)/M$:

$$\begin{aligned} h^{(\mathrm{mem})(1)}_{2\pm2} = &-\sqrt{\frac{\pi}{5}}\frac{x^5\,\eta^2\,e_t^2}{R\,(1-e_t^2)^{7/2}}\,e^{\mp 2ikv}\left[\frac{52}{21}+\frac{8}{21}e_t^2\right] \\ &-\sqrt{\frac{\pi}{5}}\frac{x^6\,\eta^2\,e_t^2}{R\,(1-e_t^2)^{9/2}}\,e^{\mp 2ikv}\Bigg[-105+\frac{1678}{9}\eta \\ &+e_t^2\left(-\frac{833}{9}+\frac{10468}{63}\eta\right)+e_t^4\left(-\frac{723}{112}+\frac{4673}{504}\eta\right)\Bigg], \end{aligned} \tag{3.52a}$$

$$h^{(\mathrm{mem})(1)}_{3\pm1} = \pm\sqrt{\frac{\pi}{70}}\frac{\eta^2\,x^{11/2}\,\Delta\,e_t}{R\,(1-e_t^2)^4}\,e^{\mp ikv}\left[\frac{2464}{45}+\frac{423}{5}e_t^2+\frac{653}{90}e_t^4\right], \tag{3.52b}$$

$$h^{(\mathrm{mem})(1)}_{3\pm3} = \mp\sqrt{\frac{\pi}{42}}\frac{\eta^2\,x^{11/2}\,\Delta\,e_t^3}{R\,(1-e_t^2)^4}\,e^{\mp 3ikv}\left[\frac{269}{45}+\frac{79}{180}e_t^2\right], \tag{3.52c}$$

$$h^{(\mathrm{mem})(1)}_{4\pm2} = -\sqrt{\pi}\frac{\eta^2\,x^5\,e_t^2}{R\,(1-e_t^2)^{7/2}}\,e^{\mp 2ikv}\left[\frac{13}{315}+\frac{2}{315}e_t^2\right] - \sqrt{\pi}\frac{x^6\,\eta^2\,e_t^2}{R\,(1-e_t^2)^{9/2}}\,e^{\mp 2ikv}\Bigg[-\frac{1151}{180}+\frac{5050}{297}\eta + e_t^2\left(-\frac{123}{20}+\frac{176921}{10395}\eta\right)+e_t^4\left(-\frac{1919}{4928}+\frac{175169}{166320}\eta\right)\Bigg], \tag{3.52d}$$

$$h^{(\mathrm{mem})(1)}_{4\pm4} = -\sqrt{\frac{\pi}{7}}\frac{5}{72}\frac{x^5\,\eta^2\,e_t^4}{R\,(1-e_t^2)^{7/2}}\,e^{\mp 4ikv} + \sqrt{\frac{\pi}{7}}\frac{x^6\,\eta^2\,e_t^4}{R\,(1-e_t^2)^{9/2}}\,e^{\mp 4ikv}\left[-\frac{16837}{3168}+\frac{841}{135}\eta+e_t^2\left(-\frac{6907}{10560}+\frac{8539}{23760}\eta\right)\right], \tag{3.52e}$$

$$h^{(\mathrm{mem})(1)}_{5\pm1} = \pm\sqrt{\frac{\pi}{77}}\frac{\eta^2\,x^{11/2}\,\Delta\,e_t}{R\,(1-e_t^2)^4}\,e^{\mp ikv}\left[\frac{43}{45}+\frac{17}{10}e_t^2+\frac{59}{360}e_t^4\right], \tag{3.52f}$$

$$h^{(\mathrm{mem})(1)}_{5\pm3} = \mp\sqrt{\frac{\pi}{66}}\frac{\eta^2\,x^{11/2}\,\Delta\,e_t^3}{R\,(1-e_t^2)^4}\,e^{\mp 3ikv}\left[\frac{31}{90}+\frac{7}{720}e_t^2\right], \tag{3.52g}$$

$$h^{(\mathrm{mem})(1)}_{5\pm5} = \mp\sqrt{\frac{5\pi}{66}}\frac{5}{48}\frac{\eta^2\,x^{11/2}\,\Delta\,e_t^5}{R\,(1-e_t^2)^4}\,e^{\mp 5ikv}, \tag{3.52h}$$

$$h^{(\mathrm{mem})(1)}_{6\pm2} = -\sqrt{\frac{\pi}{13}}\frac{x^6\,\eta^2\,e_t^2}{R\,(1-e_t^2)^{9/2}}\,e^{\mp 2ikv}\Bigg[-\frac{253}{560}+\frac{159}{110}\eta + e_t^2\left(-\frac{541}{1008}+\frac{233}{132}\eta\right)+e_t^4\left(-\frac{27}{220}+\frac{3627}{98560}\eta\right)\Bigg], \tag{3.52i}$$

$$h^{(\mathrm{mem})(1)}_{6\pm4} = -\sqrt{\frac{\pi}{390}}\frac{x^6\,\eta^2\,e_t^4}{R\,(1-e_t^2)^{9/2}}\,e^{\mp 4ikv}\left[\frac{703}{1056}-\frac{17}{8}\eta+e_t^2\left(-\frac{27}{704}+\frac{3}{22}\eta\right)\right], \tag{3.52j}$$

$$h^{(\mathrm{mem})(1)}_{6\pm6} = \sqrt{\frac{5\pi}{143}}\frac{x^6\,\eta^2\,e_t^6}{R\,(1-e_t^2)^{9/2}}\,e^{\mp 6ikv}\left[-\frac{95}{768}-\frac{5}{12}\eta\right]. \tag{3.52k}$$

The Newtonian parts of Eqs. (3.52a), (3.52d) and (3.52e) can be compared to Eqs. (2.27b,d,e) in Ref. [1]. They are in agreement, apart from an overall minus sign in the $h^{(\mathrm{mem})(1)}_{2\pm2}$ and $h^{(\mathrm{mem})(1)}_{4\pm2}$ modes. Since we will immediately explain that the $m \neq 0$ modes do not contribute to the memory, this will not make a difference for the rest of the work.

In contrast to the $m = 0$ memory modes, the $m \neq 0$ modes contain a factor e^{-imkv} due to the periastron precession. In the next step, the $h^{(\mathrm{mem})(1)}_{lm}$ have to be integrated over the entire past history of the system to find the memory contribution to the multipole modes. Since these factors cause the $m \neq 0$ modes to oscillate, the integration will suppress these modes. Instead, the $m \neq 0$ modes lead to oscillatory contributions to the full waveform entering at 2.5PN order. Therefore only the $m = 0$ modes will contribute to a secularly increasing memory effect. Moreover, the leading contributions of the $m \neq 0$ modes go with $\sim e_t^m$ and because e_t tends to get smaller and smaller as the system circularizes, this causes a further suppression. Henceforth we will concentrate on the $m = 0$ modes.

3.4 Memory contributions to the multipole modes

3.4.1 Numerically integrating the hereditary time integral

The last step to get the memory contribution to the multipole modes is to integrate the calculated time derivatives of the memory multipole modes (Eqs. (3.45), (3.48) and (3.49)) over the entire past of the system. The important effect on this timescale is radiation-reaction. Due to the emission of gravitational waves, the binary's orbit is shrinking and therefore the frequency is increasing and accordingly the post-Newtonian parameter x. On the other hand, the binary tends to lose its eccentricity and to circularize the more orbital energy it loses. To describe these effects, we can find 1PN-accurate expressions for the time evolution of x and e_t in Eq. (A2) in Ref. [52] and Eq. (6.18) in Ref. [55]. They read

$$\begin{aligned}\frac{dx}{dt} &= \frac{2\,\eta\,x^5}{15M(1-e_t^2)^{7/2}}\left(96+292e_t^2+37e_t^4\right)\\ &+\frac{\eta\,x^6}{M(1-e_t^2)^{9/2}}\Bigg(-\frac{2972}{105}-\frac{176}{5}\eta+e_t^2\left(\frac{1462}{7}-380\eta\right)\\ &+e_t^4\left(\frac{12217}{30}-\frac{1687}{5}\eta\right)+e_t^6\left(\frac{11717}{420}-\frac{296}{15}\eta\right)\Bigg),\end{aligned} \tag{3.53}$$

and

$$\begin{aligned}\frac{de_t}{dt} &= -\frac{\eta\,x^4\,e_t}{15M(1-e_t^2)^{5/2}}\left(304+121e_t^2\right)\\ &-\frac{\eta\,e_t\,x^5}{M(1-e_t^2)^{7/2}}\Bigg(-\frac{939}{35}-\frac{4084}{45}\eta\\ &+e_t^2\left(\frac{29917}{105}-\frac{7753}{30}\eta\right)+e_t^4\left(\frac{13929}{280}-\frac{1664}{45}\eta\right)\Bigg).\end{aligned} \tag{3.54}$$

This system of two coupled differential equations can be analytically solved by successive approximations, which we will do in the next section. Here we want to find x and e_t directly as a function of time, insert it into the $h_{lm}^{(\mathrm{mem})(1)}$ and perform the integral

$$h_{lm}^{(\mathrm{mem})}=\int_{-\infty}^{T_R} dt\, h_{lm}^{(\mathrm{mem})(1)}, \tag{3.55}$$

to find the memory modes. Hence we solve the evolution equations numerically between a very early time, say when the eccentricity of the system is almost 1, and a late time shortly before the merger. Because post-Newtonian theory is only valid during the inspiral phase of a binary system, we stop the integration at the last stable orbit, before the individual components plunge towards each other and eventually merge. An expression for the orbital frequency at the last stable orbit for eccentric binaries can be found in Eq. (D1) in Ref. [54]

$$n_{\mathrm{lso}}\,M = x_{\mathrm{lso}}^{3/2}=\left(\frac{1-e_t^2}{6+2e_t}\right)^{3/2}, \tag{3.56}$$

which can be solved numerically for the explicit time when the last stable orbit is reached. Note that this guess can not be valid for large eccentricities at this time, but realistic systems should have circularized enough at this point. What happens to the memory mode after the last stable orbit, during the merger and the ring-down, is discussed later in Section 3.5.2. Fig. 3.1 gives an impression how the memory modes evolve over the time of the inspiral.

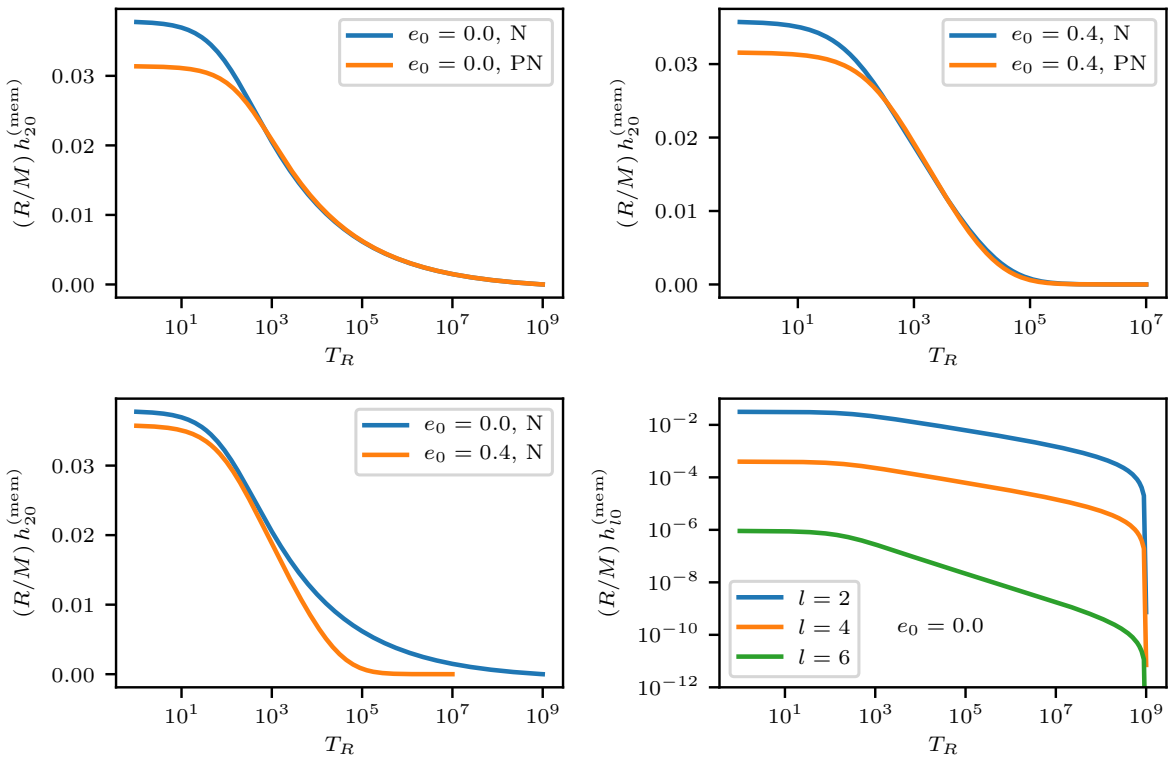

Figure 3.1: Dependence of the non-linear memory on retarded time. The time axis is shifted such that the last stable orbit of the binary system is reached at $T_R = 0$, the time then evolves into the past. All plots are for equal mass binaries, thus $\eta = 0.25$, and at the time of e_0, the value of x is $x_0 = 0.07$.
On top to the left-hand side, the buildup of memory is shown for a quasicircular binary, for the leading Newtonian order (N) and the first post-Newtonian correction (PN). On the right-hand side is the same for an eccentric system. One can see that post-Newtonian corrections tend to decrease the magnitude of the memory.
In the bottom left, the memory from a circular and an eccentric system are compared. Note that the memory begins to build up later in the eccentric system because it loses more energy in gravitational waves and is therefore less old. At the last stable orbit, the circular system has gained a little more memory than the eccentric one. In the bottom right, the non-zero memory modes in a circular system are compared. The higher modes decrease each by about two orders of magnitude.

3.4.2 Analytical solution for radiation-reaction equations

Instead of computing the integral over the entire past history of the binary system numerically, it is possible to find an analytical approximation. The time evolution equation for x (Eq. (3.53)) has to be divided by the one for e_t (Eq. (3.54)), thereby eliminating the time dependence. At leading order, a differential equation for x is obtained,

$$\frac{dx}{de_t} = -\frac{2x\left(96 + 292e_t + 37e_t^4\right)}{e_t\left(1 - e_t^2\right)\left(304 + 121e_t^2\right)}, \tag{3.57}$$

which can be integrated by separation of variables to get x as a function of e_t,

$$x_{\mathrm{N}}(e_t) = x_0 \frac{e_0^{12/19}\left(304 + 121e_0^2\right)^{870/2299}}{\left(1 - e_0^2\right)} \frac{\left(1 - e_t^2\right)}{e_t^{12/19}\left(304 + 121e_t^2\right)^{870/2299}}. \tag{3.58}$$

In this equation the subscript N indicates that we are just solving the leading Newtonian order. Initial conditions are already included such that for the eccentricity e_0, x is given by x_0.

To find the first post-Newtonian correction to Eq. (3.58), we begin again by dividing the 1PN accurate evolution equations (Eqs. (3.53) and (3.54)) and expand the right hand-side in x. This yields an equation of the form

$$\frac{dx}{de_t} = f_{\rm N}(e_t)\, x + f_{\rm PN}(e_t) x^2, \tag{3.59}$$

where $f_{\rm N}$ is the leading order part that can be read off Eq. (3.57) and $f_{\rm PN}$ is the 1PN part given by

$$\begin{aligned} f_{\rm PN}(e_t) = \frac{1}{e_t\left(1-e_t^2\right)\left(304+121e_t^2\right)^2}\Bigg[&\frac{362624}{7} - 100864\eta - e_t^2\left(\frac{1845548}{7} - \frac{469552}{3}\eta\right) \\ &+ e_t^4\left(\frac{767992}{2} - \frac{259048}{3}\eta\right) - e_t^6\left(\frac{64181}{14} - \frac{15688}{3}\eta\right)\Bigg]. \end{aligned} \tag{3.60}$$

To solve Eq. (3.59) for x consistently to the right post-Newtonian order, we need to make an expansion ansatz of the form $x(e_t) = \varepsilon\, x_{\rm N}(e_t) + \varepsilon^2\, x_{\rm PN}(e_t)$, where ε is just a dummy parameter to indicate the PN order. Inserting this ansatz into Eq. (3.59) and equating terms of the same order in ε, one finds at the leading order the Newtonian relation (Eq. (3.57)). The ε^2 terms yield

$$\frac{dx_{\rm PN}}{de_t} = f_{\rm N}(e_t)\, x_{\rm PN} + f_{\rm PN}(e_t)\, x_{\rm N}^2, \tag{3.61}$$

and higher order terms can be neglected. Since we already know $x_{\rm N}$ (Eq. (3.58)), we can insert it and then solve the differential equation for $x_{\rm PN}$ for example by the method of variation of the constant. The post-Newtonian part of $x(e_t)$ can be expressed in terms of the hypergeometric function ${}_2F_1$,

$$\begin{aligned} x_{\rm PN}(e_t) = {}& \frac{\left(1-e_t^2\right)\, C}{e_t^{12/19}\left(304+121e_t^2\right)^{870/2299}} \\ &+ \frac{x_0^2\left(1-e_t^2\right)e_0^{24/19}\left(304+121e_0^2\right)^{1740/229}}{e_t^{24/19}\left(1-e_0^2\right)^2\left(304+121e_t^2\right)^{4039/2299}}\Bigg[-\frac{5666}{21} + \frac{1576}{3}\eta \\ &+ e_t^2\left(-\frac{1555687953}{1838020} + \frac{10032850}{1929921}\eta\right) + e_t^4\left(-\frac{4472255861}{308787360} + \frac{115323167}{2205624}\eta\right) \\ &+ 2^{1118/2299}\, 19^{1429/2299}\, e_t^2\left(304+121e_t^2\right)^{3169/2299} \\ &\times\left(-\frac{37041343}{16056942720} + \frac{2627}{2940832}\eta\right) {}_2F_1\left(\frac{870}{2299}, \frac{13}{19}, \frac{32}{19}, -\frac{121e_t^2}{304}\right)\Bigg], \end{aligned} \tag{3.62}$$

and the constant C is chosen such that $x_{\rm PN}(e_0) = 0$. In this case, the Newtonian and post-Newtonian solutions for $x(e_t)$ coincide at $x(e_0) = x_0$ and one can easily compare their evolution. Note that the 1PN-accurate solution has to be constructed by $x(e_t) = x_{\rm N}(e_t) + x_{\rm PN}(e_t)$. Fig. 3.2 shows the evolution of x as a function of eccentricity e_t in an equal mass binary system. As the initially eccentric binary circularizes, it comes into the relativistic regime where the post-Newtonian solution begins to deviate from the Newtonian one and eventually, the analytical post-Newtonian solution begins to fail at $x \approx 0.3$. This is not dramatic because after the last stable orbit, which here happens at $e_t \approx 0.0022$, these equations do not describe the binary's evolution anymore and we will stop the computation of the memory there.

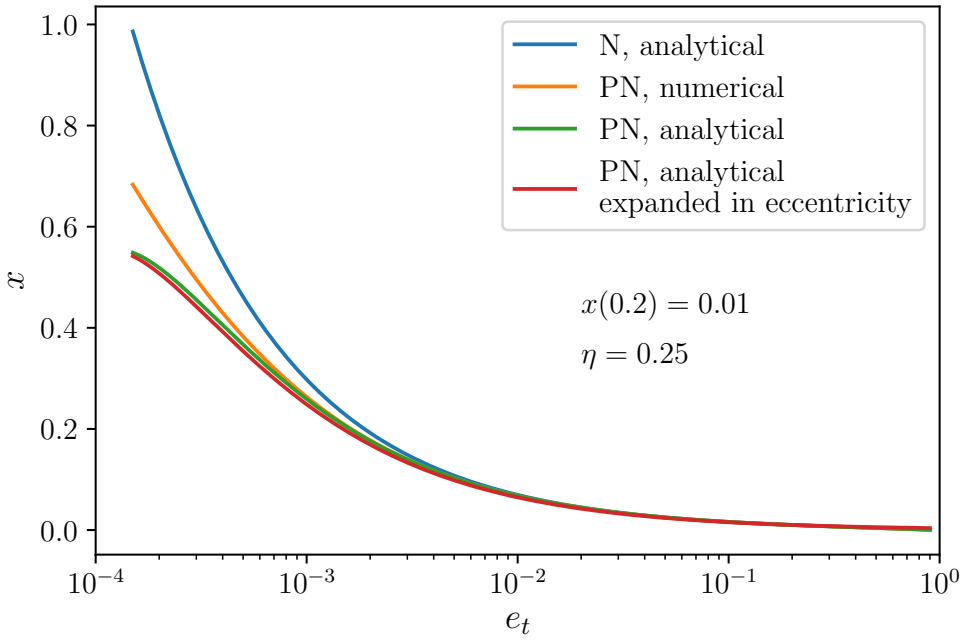

Figure 3.2: Evolution of the post-Newtonian parameter x as a function of eccentricity. In this example of an equal mass binary the initial conditions are chosen such that $x(e_0 = 0.2) = 0.01$. The blue line is the analytical Newtonian solution given by Eq. (3.58) and the orange curve represents Eq. (3.59) integrated numerically. The analytical solution given by $x(e_t) = x_{\rm N}(e_t) + x_{\rm PN}(e_t)$ is plotted in green and the lowest order eccentricity expansion of this solution is shown in red.

3.4.3 Calculating the hereditary time integral analytically

Now we are in the position to rewrite the hereditary time integral to an integral over the eccentricity of the system, which starts at some early-time value e_- and evolves due to radiation-reaction to some value $e_+ = e_t(t)$. Therefore we can write

$$h_{lm}^{(\rm mem)} = \int_{-\infty}^{T_R} dt\, h_{lm}^{(\rm mem)(1)} = \int_{e_-}^{e_t} de_t\, \frac{h_{lm}^{(\rm mem)(1)}}{de_t/dt}, \tag{3.63}$$

where for de_t/dt we can insert Eq. (3.54). The integrand is then expanded in x to get a form

$$h_{lm}^{(\rm mem)} = \int de_t \left({}^{\rm N}h_{lm}^{(\rm mem)(1)}(e_t)\, x + {}^{\rm PN}\, h_{lm}^{(\rm mem)(1)}(e_t)\, x^2 \right), \tag{3.64}$$

where ${}^{\rm N}h_{lm}^{(\rm mem)(1)}(e_t)$ is the Newtonian part and ${}^{\rm PN}h_{lm}^{(\rm mem)(1)}(e_t)$ is the post-Newtonian part of the derivatives of the memory modes as a function of eccentricity. As an example, we provide explicit expressions for the dominant $h_{20}^{(\rm mem)}$ memory mode:

$${}^{\rm N}h_{20}^{(\rm mem)(1)}(e_t) = \sqrt{\frac{10\pi}{3}} \frac{2M\,\eta}{7R} \frac{(192 + 580e_t^2 + 73e_t^4)}{e_t\,(1-e_t^2)(304 + 121e_t^2)}, \tag{3.65a}$$

$$\begin{aligned} {}^{\rm PN}h_{20}^{(\rm mem)(1)}(e_t) = \sqrt{\frac{5\pi}{6}} \frac{M\,\eta}{R} \frac{1}{e_t\,(1-e_t^2)^2(304 + 121e_t^2)^2} \Bigg[& -\frac{14261888}{147} + \frac{1055232}{7}\eta \\ & + e_t^2 \left(\frac{124216}{21} + \frac{12534}{944}\eta \right) + e_t^4 \left(-\frac{26318112}{49} + \frac{20298512}{21}\eta \right) \\ & + e_t^6 \left(-\frac{532255}{7} + \frac{4154770}{21}\eta \right) + e_t^8 \left(-\frac{810781}{49} + \frac{330403}{21}\eta \right) \Bigg]. \end{aligned} \tag{3.65b}$$

Since x itself is a function of eccentricity and consists of a Newtonian and a post-Newtonian part ($x(e_t) = x_{\rm N}(e_t) + x_{\rm PN}(e_t)$), we put it into Eq. (3.64) and only take into account terms up to 1PN order, eventually leading to an integral

$$h_{lm}^{(\rm mem)} = \int de_t \left[{}^{\rm N}h_{lm}^{(\rm mem)(1)}(e_t)\, x_{\rm N}(e_t) + {}^{\rm PN}\, h_{lm}^{(\rm mem)(1)}(e_t)\, x_{\rm N}^2(e_t) + {}^{\rm N}\, h_{lm}^{(\rm mem)(1)}(e_t)\, x_{\rm PN}(e_t) \right], \tag{3.66}$$

which consists of a purely Newtonian term and two post-Newtonian terms.

In principle, Eq. (3.66) could be integrated analytically, resulting in a complicated sum of hypergeometric functions (see Appendix B of Ref. [1], where it is done in the Newtonian case). However, since most of the memory is acquired at late times when the binary system has already circularized much, a low eccentricity expansion is justified. Expanding ${}^{\rm N}h_{20}^{(\rm mem)(1)}(e_t)$, ${}^{\rm PN}h_{20}^{(\rm mem)(1)}(e_t)$ and $x(e_t)$ in eccentricity and neglecting all terms of order $\mathcal{O}(e_t)$, we find for these terms the simple forms:

$$x_{\rm N}(e_t) = x_0 \left(\frac{e_0}{e_t}\right)^{12/19}, \tag{3.67a}$$

$$x_{\rm PN}(e_t) = x_0^2 \frac{e_0^{12/19}\left(e_0^{12/19} - e_t^{12/19}\right)}{e_t^{24/19}} \left(-\frac{2833}{3192} + \frac{197}{114}\eta\right), \tag{3.67b}$$

$${}^{\rm N}h_{20}^{(\rm mem)(1)}(e_t) = -\frac{8M\,\eta\,\sqrt{30\pi}}{133\,e_t\,R}, \tag{3.67c}$$

$${}^{\rm PN}h_{20}^{(\rm mem)(1)}(e_t) = -\sqrt{\frac{5\pi}{6}}\frac{M\,\eta}{e_t\,R}\left(-\frac{111421}{106134} + \frac{4122}{2527}\eta\right). \tag{3.67d}$$

In this low eccentricity expansion, the calculation of the hereditary integral given by Eq. (3.63) is straightforward and yields for the Newtonian and post-Newtonian part

$${}^{\rm N}h_{20}^{(\rm mem)} = \frac{2}{7}\sqrt{\frac{10\pi}{3}}\frac{M\,\eta\,x_0}{R}\left[\left(\frac{e_0}{e_t}\right)^{12/19} - \left(\frac{e_0}{e_-}\right)^{12/19}\right], \tag{3.68a}$$

$$\begin{aligned} {}^{\rm PN}h_{20}^{(\rm mem)} = \sqrt{\frac{5\pi}{6}}\frac{M\,\eta\,x_0^2}{R}\Bigg[&\left(-\frac{2833}{5586} + \frac{394}{399}\eta\right)\left(\left(\frac{e_0}{e_m}\right)^{12/19} - \left(\frac{e_0}{e_t}\right)^{12/19}\right) \\ &+ \left(-\frac{145417}{134064} + \frac{407}{228}\eta\right)\left(\left(\frac{e_0}{e_t}\right)^{24/19} - \left(\frac{e_0}{e_-}\right)^{24/19}\right)\Bigg]. \end{aligned} \tag{3.68b}$$

We can insert back the result for $x(e_t)$ in order to eliminate the constants x_0 and e_0. Again one has to be aware of putting in the correct post-Newtonian orders. The memory mode then becomes

$$\begin{aligned} h_{20}^{(\rm mem)} = \frac{2}{7}\sqrt{\frac{10\pi}{3}}\frac{\eta\,M\,x}{R}\Bigg\{1 &- \left(\frac{e_t}{e_-}\right)^{12/19} \\ &+ x\left[\left(-\frac{2833}{3192} + \frac{197}{114}\eta\right)\left(\frac{e_t}{e_-}\right)^{12/19} + \left(-\frac{4075}{4032} + \frac{67}{48}\eta\right)\right]\Bigg\}, \end{aligned} \tag{3.69}$$

where one can easily recognize Newtonian and post-Newtonian orders. The Newtonian term can be compared to Eq. (2.35a) in Ref. [1] under the change from p to $x = M/p$, and they are in agreement. It is also no problem to take the circular limit of Eq. (3.69), one simply has to set $e_t = 0$. Newtonian and 1PN part can then be compared to Eq. (4.3a) in Ref. [48] and are found to be equal.

In Fig. 3.3 the $h_{20}^{(\rm mem)}$ mode is plotted as a function of eccentricity. On the left-hand side we show the Newtonian and the 1PN-accurate mode for three reference eccentricities. The evolution

of the mode is stopped when the binary attains its last stable orbit as defined in Eq. (3.56). What happens to the memory in the merger and the ringdown is shortly discussed for binary black holes in Section 3.5.2. Since the more eccentric orbits emit more gravitational radiation, they evolve faster on the radiation-reaction timescale and therefore have less time to gain memory. One can also recognize that the post-Newtonian correction tends to decrease the memory as the orbit shrinks and consequently becomes more relativistic.

On the right-hand side in Fig. 3.3 we compare the low eccentricity expansion to the full solution obtained by numerically integrating Eq. (3.66). If the computation of the memory is started at a small value (brown curve, $e_- = 0.1$), they agree almost perfectly. At higher eccentricity values, the mismatch becomes larger and one has to either expand to higher orders in eccentricity, or take the full solution. But notice that most of the memory is built up at small eccentricities and on the other hand most real compact binaries are observed to have insignificant eccentricities [56].

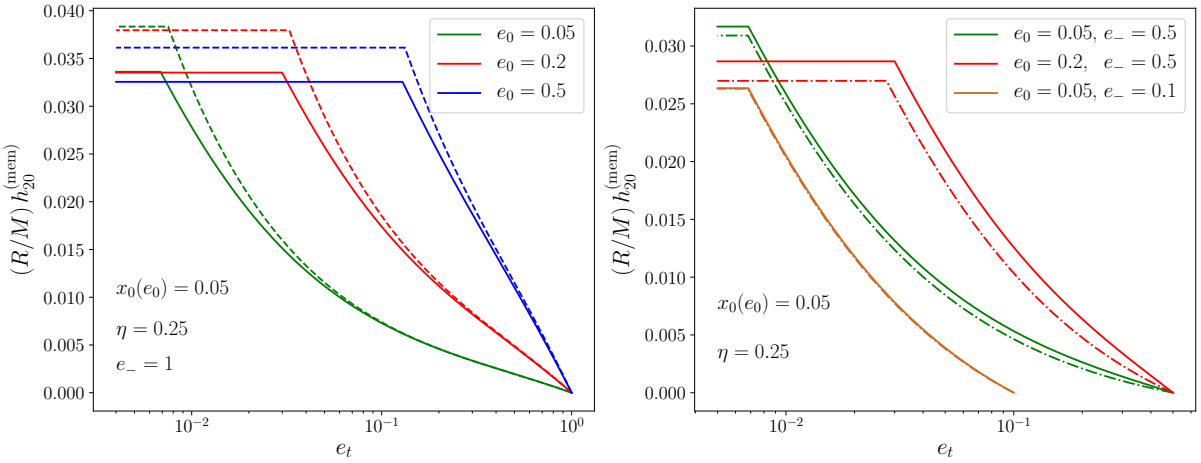

Figure 3.3: Both plots show the dominating $h_{20}^{(\mathrm{mem})}$ memory mode as a function of eccentricity e_t for different values of the reference eccentricity e_0. This means all curves pass through $e_t = e_0$ when $x = x_0$. We have stopped the integration as soon as the last stable orbit is reached and from this point continued the curve horizontally to compare the total memory built up in the inspiral phase. On the left, the dashed lines show the Newtonian mode and the solid lines the 1PN-accurate mode. One can see that the post-Newtonian correction diminishes the memory substantially. The right plot shows the comparison between the full solution (solid) and the low-eccentricity expansion (dash-dotted). Most of the deviation builds up at the beginning of the integration, the more the system circularizes, the more accurate it becomes. For the brown curve, starting at already low eccentricity, it matches almost perfectly.

Using the same procedure, we are able to calculate $h_{40}^{(\mathrm{mem})}$ and $h_{60}^{(\mathrm{mem})}$ in the low eccentricity limit. Their respective Newtonian and post-Newtonian parts are given by:

$$ {}^{\mathrm{N}}h_{40}^{(\mathrm{mem})} = \frac{1}{63}\sqrt{\frac{\pi}{10}}\frac{M\,\eta\,x_0}{R}\left[\left(\frac{e_0}{e_t}\right)^{12/19} - \left(\frac{e_0}{e_-}\right)^{12/19}\right], \tag{3.70a} $$

$$
\begin{aligned}
{}^{\mathrm{PN}}h_{40}^{(\mathrm{mem})} = \sqrt{\frac{\pi}{10}}\frac{M\,\eta\,x_0^2}{R}\Bigg[&\left(-\frac{1223741}{11797632}+\frac{534649}{1264032}\eta\right)\left(\left(\frac{e_0}{e_t}\right)^{24/19}-\left(\frac{e_0}{e_-}\right)^{24/19}\right)\\
&+\left(-\frac{2833}{402192}+\frac{197}{14364}\eta\right)\Bigg(\left(\frac{e_0}{e_t}\right)^{24/19}-\left(\frac{e_0}{e_-}\right)^{24/19}\\
&+2\left(\frac{e_0}{e_-}\right)^{12/19}-2\left(\frac{e_0}{e_t}\right)^{12/19}\Bigg)\Bigg],
\end{aligned}
\tag{3.70b}
$$

$$
{}^{\mathrm{N}}h_{60}^{(\mathrm{mem})} = 0, \tag{3.70c}
$$

$$
{}^{\mathrm{PN}}h_{60}^{(\mathrm{mem})} = \sqrt{\frac{5\pi}{273}}\frac{M\,\eta\,x_0^2}{R}\left(-\frac{839}{177408}+\frac{43}{2112}\eta\right)\left(\left(\frac{e_0}{e_-}\right)^{24/19}-\left(\frac{e_0}{e_t}\right)^{24/19}\right). \tag{3.70d}
$$

Expressing these modes again in terms of x yields

$$
\begin{aligned}
h_{40}^{(\mathrm{mem})} = \frac{1}{63}\sqrt{\frac{\pi}{10}}\frac{\eta\,M\,x}{R}\Bigg\{&1-\left(\frac{e_t}{e_-}\right)^{12/19}\\
&+x\left[\left(-\frac{2833}{3192}+\frac{197}{228}\eta\right)\left(\frac{e_t}{e_-}\right)^{12/19}+\left(-\frac{180101}{29568}+\frac{27227}{1056}\eta\right)\right]\Bigg\},
\end{aligned}
\tag{3.71a}
$$

$$
h_{60}^{(\mathrm{mem})} = \sqrt{\frac{5\pi}{273}}\frac{\eta\,M\,x^2}{R}\left(-\frac{839}{177408}+\frac{43}{2112}\eta\right). \tag{3.71b}
$$

The circular limit of these memory modes can be compared to Eq. (4.3b) and (4.3c) in Ref. [48]. Since in Eq. (3.71b) the eccentricity dependence has vanished to the lowest order due to the expansion, we add back the leading order eccentricity term, so that it reads

$$
h_{60}^{(\mathrm{mem})} = \sqrt{\frac{5\pi}{273}}\frac{\eta\,M\,x^2}{R}\left(-\frac{839}{177408}+\frac{43}{2112}\eta\right)\left(1-\left(\frac{e_t}{e_-}\right)^{24/19}\right), \tag{3.72}
$$

just to show how the eccentricity modifies the circular limit.

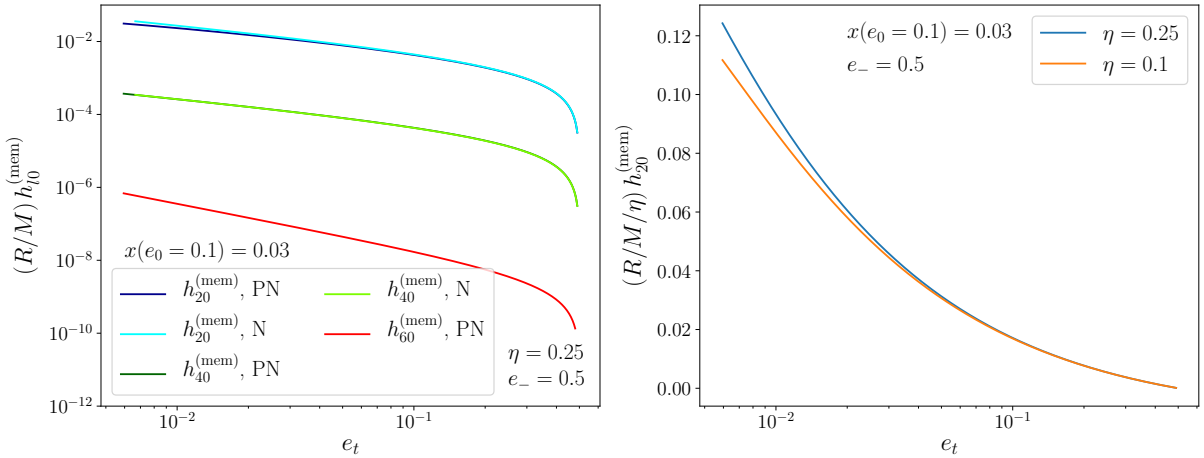

Figure 3.4: The left plot shows the memory modes for $l=2,4,6$ as a function of eccentricity. The plot on the right presents the $h_{20}^{(\mathrm{mem})}$-mode for two different values of the symmetric mass ratio η. Note that we have divided the mode by η to concentrate on the difference in the memory. The η in front would act on the whole waveform and therefore suppress it for unequal mass binaries.

Fig. 3.4 shows the order of magnitude of the different l memory modes given in Eqs. (3.69), (3.71a) and (3.71b). The $l = 2$ mode is clearly predominant and one can also discern the post-Newtonian correction at late times. On the right-hand side we show the dependence of the dominant mode on the symmetric mass ratio η. The gained memory is considerably higher for equal mass binaries, which have $\eta = 0.25$, than for a binary system with $\eta = 0.1$, which would for example correspond to 5 and 40 solar masses respectively for the individual components.

3.5 Memory in the waveform

3.5.1 Memory from the inspiral

We now have essentially three modes that contribute to the gravitational wave memory effect up to 1PN order. With the help of Eq. (3.11) we can calculate the waveform polarizations. It is verified quickly, that the non-linear memory affects the plus polarization only. This is mainly a consequence of our choice of the polarization triad. A rotation of the polarization triad would cause a purely plus-polarized wave to become mixed-polarized. Calculating the plus-polarization from the multipoles, we can write it in the following form,

$$h_+^{(\mathrm{mem})} = \frac{2\eta\, M\, x}{R}\left({}^{\mathrm{N}}H_+^{(\mathrm{mem})} + x\ {}^{\mathrm{PN}}H_+^{(\mathrm{mem})}\right), \tag{3.73}$$

where in the low eccentricity limit the Newtonian part reads

$${}^{\mathrm{N}}H_+^{(\mathrm{mem})} = \frac{1}{96}\sin^2\Theta\left(17+\cos^2\Theta\right)\left(1-\left(\frac{e_t}{e_-}\right)^{12/19}\right), \tag{3.74}$$

and the post-Newtonian part is

$$\begin{aligned}{}^{\mathrm{PN}}H_+^{(\mathrm{mem})} = \sin^2\Theta\Bigg[&-\frac{354241}{2064384}+\frac{15607}{73728}\eta+\left(-\frac{48161}{306432}+\frac{3349}{10944}\eta\right)\left(\frac{e_t}{e_-}\right)^{12/19}\\ &+\cos^2\Theta\left(-\frac{62059}{1032192}+\frac{9373}{36864}\eta+\left(-\frac{2833}{306432}+\frac{197}{10944}\right)\left(\frac{e_t}{e_-}\right)^{12/19}\right)\\ &+\cos^4\Theta\left(-\frac{4195}{688128}+\frac{215}{8192}\eta\right)\Bigg].\end{aligned} \tag{3.75}$$

Once more we can compare the circular limit to the explicit expressions given by Favata [48] in his Eqs. (4.4-4.6), and they are in perfect agreement.

3.5.2 Memory from merger and ringdown of binary black holes

The calculation of the memory we have done so far only takes into account the inspiral phase where the post-Newtonian formalism is valid. However, the emission of gravitational waves is greatest in the merger, so one can expect that much more memory will accumulate in the late phase of the coalescence. For the computation of the waveform at these stages, numerical relativity simulations are used, nevertheless the calculation of the memory in these simulations faces some difficulties. They can best resolve the $l = m = 2$ mode of the waveform, but the memory appears only in the $m = 0$ modes, which tend to be smaller by orders of magnitude and depend sensitively on the initial conditions of the simulations [48].

Another approach to compute the memory from the entire coalescence, is to take a simple analytic model for the inspiral, merger and ringdown, the so called minimal waveform model

(MWM). It uses information from numerical relativity and the effective-one-body (EOB) approach [57] to match the leading order inspiral waveform to a sum of quasi-normal modes representing the ringdown. Following Refs. [58, 59], for the coalescence of quasicircular binary black holes, the $q^{\rm th}$ time derivative of the dominant mode is approximated as

$$h^{(q)}_{2\pm2} \approx \frac{I^{(q+2)}_{2\pm2}}{R\sqrt{2}} = \frac{1}{R\sqrt{2}} \times \begin{cases} 2\sqrt{\frac{2\pi}{5}}\eta M r^2 (\mp 2i\omega)^{q+2} e^{\mp 2i\varphi} & \text{for } t \le t_m \\ \sum_{n=0}^{n_{\rm max}} (-\sigma_{22n})^q A_{22n} e^{-\sigma_{22n}(t-t_m)} & \text{for } t > t_m, \end{cases} \tag{3.76}$$

where $I_{2\pm2}$ is the spherical harmonic coefficient of the source mass quadrupole, $\omega = \dot{\varphi} = (M/r^3)^{1/2}$, $r = r_m[1-(t-t_m)/\tau_{rr}]^{1/4}$, $\tau_{rr} = (5/256)(M/\eta)(r_m/M)^4$, $\sigma_{lmn} = i\omega_{lmn} + \tau^{-1}_{lmn}$ are the black hole quasi-normal modes and damping times depending on the remnant black hole mass and spin [60], and t_m is the matching time at which $r = r_m$. The matching radius r_m is an adjustable parameter determining the peak of the waveform amplitude, one usually chooses $r_m = 3M$ corresponding to the Schwarzschild light ring. Finally the coefficients A_{lmn} are determined by matching the two pieces at $t = t_m$.

The memory contribution to the h_{20} mode can be calculated using Eq. (3.27). In computing the leading order piece of the memory for quasicircular orbits, only the h_{22} mode is needed. Thus, the memory contribution to the waveform polarization h_+ is

$$h^{(\rm mem)}_{+} \approx \frac{R}{192\pi} \sin^2\Theta(17+\cos^2\Theta) \int_{-\infty}^{T_R} dt\, |\dot{h}_{22}|^2. \tag{3.77}$$

Substituting in the minimal waveform model given in Eq. (3.76) and evaluating the integral yields a relatively simple analytical expression for the evolution of the memory,

$$\begin{aligned} h^{(\rm mem)}_{+,\rm MWM} \approx \frac{\eta\, M}{384\pi R} \sin^2\Theta(17+\cos^2\Theta) \Bigg\{ & \frac{8\pi M}{r(T)} H(-T) \\ & + \left[\frac{8\pi M}{r_m} + \frac{1}{\eta M} \sum_{n,n'=0}^{n_{\rm max}} \frac{\sigma_{22n}\sigma^*_{22n'}}{\sigma_{22n}+\sigma^*_{22n'}} A_{22n} A^*_{22n'} \left(1 - e^{-(\sigma_{22n}+\sigma^*_{22n'})T}\right) \right] H(T) \Bigg\}, \end{aligned} \tag{3.78}$$

where $H(T)$ denotes the Heaviside function. One could further improve this model by using an EOB description of the h_{22} mode and substitute it into Eq. (3.77). Fig. 3.5 (taken from Ref. [58]) shows the h_+ polarization generated during the coalescence of two equal mass black holes with and without memory contribution. This was calculated using the full EOB model.

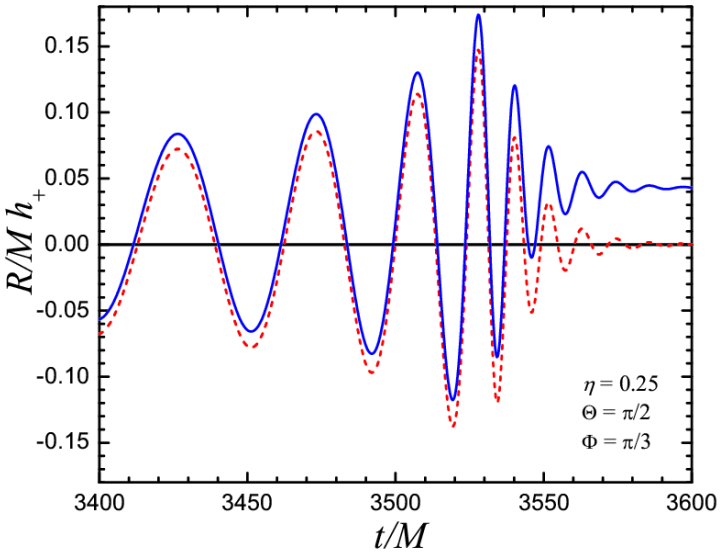

Figure 3.5: The plus-polarization waveform from the late phase inspiral, merger and ringdown of a binary black hole coalescence computed using a full effective-one-body model with (solid, blue) and without (dashed, red) memory. (Figure from Ref. [58])

3.6 Detecting the memory

After the first direct observations of gravitational wave signals, it is legitimate to ask if also the imprint of the memory is observable. The memory itself from a gravitational wave passing through spacetime in the distant past long before the observation is undetectable. It would simply correspond to an unobservable constant shift in the Minkowski metric.

Nonetheless, what is observable, is the accumulation of memory over time as the gravitational waves pass through the detector. A simple estimate of the detectability of the memory with gravitational wave interferometers is done by calculating the sky-averaged rms signal-to-noise ratio (SNR),

$$\mathrm{SNR} = \left[\int_0^\infty \frac{df}{f}\frac{h_c^2(f)}{h_n^2(f)}\right]^{1/2}, \tag{3.79}$$

where noise amplitude $h_n(f)$ and the memory amplitude $h_c(f)$ are given by

$$h_n(f) = \sqrt{\alpha f S_n(f)}, \tag{3.80a}$$

$$h_c(f) = 2(1+z) f \langle |\tilde{h}_+^{(\mathrm{mem})}[(1+z)f]|^2\rangle^{1/2}|_{R\to D_L/(1+z)}. \tag{3.80b}$$

In Eq. (3.80a), $S_n(f)$ is the noise spectral density of the detector and $\alpha = 5$ for interferometers like LIGO or $\alpha = 20/3$ for space-based detectors like LISA [61, 62]. In Eq. (3.80b), $\tilde{h}_+^{(\mathrm{mem})}$ denotes the Fourier transform of $h_+^{(\mathrm{mem})}$, z is the redshift, $D_L(z)$ is the luminosity distance and the angle brackets imply to average over polarization angles and sky positions.

Comparing the SNR to sensitivity curves of current or future detectors, one can estimate the chance of detecting the memory. For advanced LIGO the prospects are rather poor. It would need a binary black hole coalescence of two $50\,M_\odot$ black holes at 20 Mpc to yield a significant SNR ≈ 8. LISA is in a much better position to detect the memory of supermassive binary black hole mergers. A merger of two $10^5\,M_\odot$ black holes at $z = 2$ has an SNR of ≈ 9 [63]. Note also that ignoring memory contributions from merger and ringdown would substantially underestimate the SNR, while using the simplest imaginable model for the memory, which is just a step function, would overestimate the SNR.

4 Conclusion

Before coming to the end, we will shortly recap what has been done, state some problems and difficulties and suggest possible extensions.

4.1 Waveform polarizations in terms of Hansen coefficients

On the one hand, we have derived a formula to explicitly calculate expressions for the PN-accurate Hansen coefficients in terms of the eccentricity e_t, symmetric mass ratio η, PN parameter x and periastron advance angle δl. On the other hand, we have written the waveform polarization states $h_{+,\times}$ as a sum over harmonics of the mean anomaly l with coefficients involving the Hansen coefficients. We have explicitly written the coefficients up to 1PN order. Invoking the Hansen coefficients in the waveforms at 2PN order [12] and the instantaneous parts at 3PN order [51] would be feasible.

Furthermore, we have discussed an analytical method to calculate the Fourier transform of the waveform, the stationary phase approximation (SPA). Applying the SPA is possible because the waveform is varying on three different timescales. Amplitude and frequency evolve on the radiation-reaction timescale, the phase on the orbital timescale, and in between there is a timescale corresponding to the periastron precession. In our computation of the Fourier transform we have ignored the periastron precession, with the help of Ref. [24] it could be incorporated.

4.2 Gravitational wave memory from eccentric binaries

The non-linear gravitational wave memory effect is itself an interesting feature of the non-linearity in general relativity. Moreover, it is potentially directly observable with a gravitational wave detector like LISA.

We have investigated the gravitational wave memory effect from eccentric binary inspirals. To the leading order calculations done in Ref. [1] we have computed the 1PN corrections. In the low eccentricity limit, explicit expressions for the memory contribution to the relevant multipoles are derived in Eqs. (3.69), (3.71a) and (3.71b). An extension to 3PN order should be straightforward, in Eq. (3.27) one would insert the 3PN-accurate $\dot{h}_{lm}$ and follow the same steps as have been done in Sections 3.3 and 3.4, but expanding each time to 3PN order.

A point that remains somewhat unclear is what happens to the $m \neq 0$ memory modes derived in Section 3.3.4. We have argued that they are not contributing to a secularly increasing memory effect, because the hereditary integral leads to a suppression due to the oscillations from the periastron precession term. It has to be further investigated if these memory modes exactly vanish or if there is still some contribution at a higher PN order.

Alongside, one should also improve the calculation of the memory accumulated during the late inspiral and the merger of binary systems, since it will contribute the most. However, this is difficult in the highly relativistic environment of the coalescence and is most likely a task for numerical relativity together with the effective-one-body formalism.

In principal, the memory effect could be used to test general relativity. It would therefore also be interesting if there is a notion of something like a memory effect in alternative theories of gravity.

A Expressions for some Fourier coefficients

Here we provide explicit expressions for some coefficients appearing in the Fourier series expansions in Sections 2.2.2 and 2.2.3. They are all extracted from Ref. [14], where also a solution to the 3PN-accurate Kepler equation, relating the mean anomaly l and the eccentric anomaly u, is derived. This solution is given in terms of the Bessel functions of the first kind J_s and reads

$$u = \sum_{s=1}^{\infty} A_s \sin(sl), \tag{A.1a}$$

$$A_s = \frac{2}{s} J_s(se_t) + \sum_{j=1}^{\infty} \alpha_j \left[J_{s+j}(se_t) - J_{s-j}(se_t) \right], \tag{A.1b}$$

where the α_j are given by

$$\begin{aligned} \alpha_j = 2\beta_\phi^j \frac{\sqrt{1-e_\phi^2}}{e_\phi^3} \Bigg[& (f_{4t} + f_{6t}) e_\phi^2 + \frac{(g_{4t} + g_{6t}) e_\phi^3}{j\sqrt{1-e_\phi^2}} + 2 i_{6t} e_\phi \left(j\sqrt{1-e_\phi^2} - 1 \right) \\ & + h_{6t} \left(4 - e_\phi^2 - 6j\sqrt{1-e_\phi^2} + 2j^2(1-e_\phi^2) \right) \Bigg]. \end{aligned} \tag{A.2}$$

The $f_{4t}, g_{4t}, ...$ are orbital functions of angular momentum and energy (see Ref. [16] for explicit expressions), e_ϕ is some angular eccentricity appearing at 1PN order and $\beta_\phi = \left(1 - \sqrt{1-e_\phi^2}\right)/e_\phi$. Expressions for α_j in terms of eccentricity, symmetric mass ratio and post-Newtonian parameter are provided in harmonic and ADM type gauges in Eq. (18) of Ref. [14].

Next we turn to the coefficients of the series expansion of $(1 - e\cos u)^n$ valid for negative n, which are given in terms of the hypergeometric function ${}_2F_1$,

$$(1 - e\cos u)^n = \sum_{j=0}^{\infty} b_j^{-n} \cos(ju), \tag{A.3a}$$

$$b_0^n = {}_2F_1\left(\frac{n}{2}, \frac{n+1}{2}; 1; e^2 \right), \tag{A.3b}$$

$$b_j^n = \frac{e^j}{2^{j-1}} \binom{n+j-1}{j} {}_2F_1\left(\frac{n+j}{2}, \frac{n+j+1}{2}; j+1; e^2 \right). \tag{A.3c}$$

From the solution of the Kepler equation, the coefficients for the expansion of trigonometric functions of u into harmonic series of l can be derived. For sine, cosine and exponentials they are

$$\sin(ju) = \sum_{s=1}^{\infty} \sigma_s^{ju} \sin(sl), \tag{A.4a}$$

$$\begin{aligned} \sigma_s^{ju} = & \frac{j}{s} \left[J_{s+j}(se_t) + J_{s-j}(se_t) \right] \\ & + \frac{j}{2} \sum_{i=1}^{\infty} \alpha_j \left[J_{s+j+i}(se_t) - J_{s+j-i}(se_t) + J_{s-j+i}(se_t) - J_{s-j-i}(se_t) \right], \end{aligned} \tag{A.4b}$$

$$\cos(ju) = \sum_{s=1}^{\infty} \zeta_s^{ju} \cos(sl), \tag{A.4c}$$

$$\zeta_0^{ju} = \frac{1}{2}\left(-e_t\delta_{j1} + \alpha_j j\right), \tag{A.4d}$$

$$\begin{aligned}\zeta_s^{ju} = {} & \frac{j}{s}\left[J_{s-j}(se_t) - J_{s+j}(se_t)\right] \\ & + \frac{j}{2}\sum_{i=1}^{\infty}\alpha_j\left[J_{s-j+i}(se_t) - J_{s-j-i}(se_t) - J_{s+j+i}(se_t) + J_{s+j-i}(se_t)\right],\end{aligned} \tag{A.4e}$$

$$e^{iju} = \sum_{s=-\infty}^{\infty} \epsilon_s^{ju} e^{(isl)}, \tag{A.4f}$$

$$\epsilon_0^{ju} = \frac{1}{2}\left(-e_t\delta_{j1} + \alpha_j j\right), \tag{A.4g}$$

$$\epsilon_s^{ju} = \frac{j}{s}J_{s-j}(se_t) + \frac{j}{2}\sum_{k=1}^{\infty}\alpha_k\left[J_{s-j+k}(se_t) - J_{s-j-k}(se_t)\right]. \tag{A.4h}$$

Trigonometric functions of the true anomaly v can be related to the eccentric anomaly via the series expansion

$$e^{ijv} = \sum_{n=0}^{\infty} \mathcal{E}_n^j e^{inu}, \tag{A.5a}$$

$$\mathcal{E}_0^j = (-\beta)^j, \tag{A.5b}$$

$$\mathcal{E}_{n>0}^j = \binom{n-1}{n-j} {}_2F_1\left(-j, n; n-j+1; \beta^2\right)\beta^{n-j}. \tag{A.5c}$$

B PN waveform in terms of Hansen coefficients

Here we give expressions for the coefficients $Q_s^{+\times}$ at half and one PN order just as it was done at Newtonian order in Eqs. (2.28c) and (2.28d). We use the abbreviations, $\Delta = (m_1 - m_2)/M$, $c_\Theta = \cos\Theta$ and $s_\Theta = \sin\Theta$. The coefficients at half PN order read:

$$\begin{aligned} Q_s^{+\,(1/2)} = \sum_{j=-\infty}^{\infty} \frac{\Delta\, s_\Theta}{8}\Big\{ & (1+c_\Theta^2)\sqrt{1-e_t^2}\Big[(9-5e_t^2)\delta_{s-j,0} - \frac{7e_t}{2}\left(\epsilon_{s-j}^{-1u} + \epsilon_{s-j}^{1u}\right) \\ & + \frac{3e_t^2}{2}\left(\epsilon_{s-j}^{-2u} + \epsilon_{s-j}^{2u}\right)\Big]\left(X_j^{-3,-3} + X_j^{-3,3}\right) - (1+c_\Theta^2)\frac{e_t}{4}\Big[(20-15e_t^2)\left(\epsilon_{s-j}^{-1u} - \epsilon_{s-j}^{1u}\right) \\ & - 4e_t\left(\epsilon_{s-j}^{-2u} - \epsilon_{s-j}^{2u}\right) + e_t^2\left(\epsilon_{s-j}^{-3u} - \epsilon_{s-j}^{3u}\right)\Big]\left(X_j^{-3,-3} - X_j^{-3,3}\right) \\ & + \sqrt{1-e_t^2}\left[e_t(3c_\Theta^2-1)\left(\epsilon_{s-j}^{-1u} + \epsilon_{s-j}^{1u}\right) - (c_\Theta^2+5)\delta_{s-j,0}\right]\left(X_j^{-2,-1} + X_j^{-2,1}\right) \\ & + (3c_\Theta^2-1)e_t\left(\epsilon_{s-j}^{-1u} - \epsilon_{s-j}^{1u}\right)\left(X_j^{-1,-1} - X_j^{-1,1}\right)\Big\}, \end{aligned} \tag{B.1a}$$

$$\begin{aligned} Q_s^{\times\,(1/2)} = \sum_{j=-\infty}^{\infty} \frac{i\Delta s_\Theta c_\Theta}{4}\Big\{ & \frac{e_t}{4}\Big[(-20+15e_t^2)\left(\epsilon_{s-j}^{-1u} - \epsilon_{s-j}^{1u}\right) + 4e_t\left(\epsilon_{s-j}^{-2u} - \epsilon_{s-j}^{2u}\right) \\ & - e_t^2\left(\epsilon_{s-j}^{-3u} - \epsilon_{s-j}^{3u}\right)\Big]\left(X_j^{-3,-3} + X_j^{-3,3}\right) + \sqrt{1-e_t^2}\Big[(9-5e_t^2)\delta_{s-j,0} \\ & - \frac{7e_t}{2}\left(\epsilon_{s-j}^{-1u} + \epsilon_{s-j}^{1u}\right) + \frac{3e_t^2}{2}\left(\epsilon_{s-j}^{-2u} + \epsilon_{s-j}^{2u}\right)\Big]\left(X_j^{-3,-3} - X_j^{-3,3}\right) \\ & + \sqrt{1-e_t^2}\Big[e_t\left(\epsilon_{s-j}^{-1u} + \epsilon_{s-j}^{1u}\right) - 3\delta_{s-j,0}\Big]\left(X_j^{-2,-1} - X_j^{-2,1}\right) \\ & + e_t\left(\epsilon_{s-j}^{-1u} - \epsilon_{s-j}^{1u}\right)\left(X_j^{-1,-1} + X_j^{-1,1}\right)\Big\}. \end{aligned} \tag{B.1b}$$

The coefficients at one PN order are given by:

$$
\begin{aligned}
Q_s^{+\,(1)} = \sum_{j=-\infty}^{\infty} \frac{1}{24}\Big\{ & - s_\Theta^2(1+c_\Theta^2)(1-3\eta)\sqrt{1-e_t^2}\frac{3e_t}{4}\Big[(-26+14e_t^2)\left(\epsilon_{s-j}^{-1u}-\epsilon_{s-j}^{1u}\right) \\
& + 9e_t\left(\epsilon_{s-j}^{-2u}-\epsilon_{s-j}^{2u}\right) - 2e_t^2\left(\epsilon_{s-j}^{-3u}-\epsilon_{s-j}^{3u}\right)\Big]\left(X_j^{-4,-4}-X_j^{-4,4}\right) \\
& + \frac{1}{8}s_\Theta^2(1+c_\Theta^2)(1-3\eta)\Big[(-256+346e_t^2-105e_t^4)\delta_{s-j,0} \\
& + (130e_t-111e_t^3)\left(\epsilon_{s-j}^{-1u}+\epsilon_{s-j}^{1u}\right) + (-61e_t^2+42e_t^4)\left(\epsilon_{s-j}^{-2u}+\epsilon_{s-j}^{2u}\right) \\
& + 9e_t^3\left(\epsilon_{s-j}^{-3u}+\epsilon_{s-j}^{3u}\right) - \frac{3e_t^4}{2}\left(\epsilon_{s-j}^{-4u}+\epsilon_{s-j}^{4u}\right)\Big]\left(X_j^{-4,-4}+X_j^{-4,4}\right) \\
& - \frac{e_t}{\sqrt{1-e_t^2}}\Big[3c_\Theta^4\Big((-5+5e_t^2+15\eta-15e_t^2\eta)\left(\epsilon_{s-j}^{-1u}-\epsilon_{s-j}^{1u}\right) \\
& + (-2e_t+2e_t^3+6\eta e_t-6e_t^3\eta)\left(\epsilon_{s-j}^{-2u}-\epsilon_{s-j}^{2u}\right)\Big) + c_\Theta^2\Big((6+30e_t^2-32\eta+20e_t^2\eta) \\
& \times\left(\epsilon_{s-j}^{-1u}-\epsilon_{s-j}^{1u}\right) + (-15e_t-3e_t^3+19e_t\eta-13e_t^3\eta)\left(\epsilon_{s-j}^{-2u}-\epsilon_{s-j}^{2u}\right)\Big) \\
& - (3-39e_t^2+32\eta+7e_t^2\eta)\left(\epsilon_{s-j}^{-1u}-\epsilon_{s-j}^{1u}\right) \\
& - (9e_t+9e_t^3-e_t\eta-5e_t^3\eta)\left(\epsilon_{s-j}^{-2u}-\epsilon_{s-j}^{2u}\right)\Big]\left(X_j^{-3,-2}-X_j^{-3,2}\right) \\
& + \Big[c_\Theta^4\Big((-8+6e_t^2+24\eta-18e_t^2\eta)\delta_{s-j,0} + (13e_t-\frac{15}{2}e_t^3-39e_t\eta+\frac{45}{2}e_t^3\eta)\left(\epsilon_{s-j}^{-1u}+\epsilon_{s-j}^{1u}\right) \\
& - (6e_t^2-18e_t^2\eta)\left(\epsilon_{s-j}^{-2u}+\epsilon_{s-j}^{2u}\right) + (\frac{3}{2}e_t^3-\frac{9}{2}e_t^3\eta)\left(\epsilon_{s-j}^{-3u}+\epsilon_{s-j}^{3u}\right)\Big) \\
& + \frac{1}{1-e_t^2}c_\Theta^2\Big((36+78e_t^2-90e_t^4+44\eta-138e_t^2\eta+94e_t^4\eta)\delta_{s-j,0} \\
& - (69e_t-\frac{177}{4}e_t^3-\frac{15}{4}e_t^5-51e_t\eta+\frac{269}{4}e_t^3\eta-\frac{65}{4}e_t^5\eta)\left(\epsilon_{s-j}^{-1u}+\epsilon_{s-j}^{1u}\right) \\
& - (-9e_t^2-3e_t^4+13e_t^2\eta-13e_t^4\eta)\left(\epsilon_{s-j}^{-2u}+\epsilon_{s-j}^{2u}\right) - (\frac{9}{4}e_t^3-\frac{3}{4}e_t^5-\frac{13}{4}e_t^3\eta+\frac{13}{4}e_t^5\eta) \\
& \times\left(\epsilon_{s-j}^{-3u}+\epsilon_{s-j}^{3u}\right)\Big) + \frac{1}{1-e_t^2}\Big((76-4e_t^2-48e_t^4-76\eta+144e_t^2\eta-32e_t^4\eta)\delta_{s-j,0} \\
& - (56e_t-\frac{95}{4}e_t^3-\frac{45}{4}e_t^5-12e_t\eta+\frac{23}{4}e_t^3\eta+\frac{25}{4}e_t^5\eta)\left(\epsilon_{s-j}^{-1u}+\epsilon_{s-j}^{1u}\right) \\
& - (-3e_t^2-9e_t^4-5e_t^2\eta+5e_t^4\eta)\left(\epsilon_{s-j}^{-2u}+\epsilon_{s-j}^{2u}\right) \\
& - (\frac{3}{4}e_t^3+\frac{9}{4}e_t^5+\frac{5}{4}e_t^3\eta-\frac{5}{4}e_t^5\eta)\left(\epsilon_{s-j}^{-3u}+\epsilon_{s-j}^{3u}\right)\Big)\Big]\left(X_j^{-3,-2}+X_j^{-3,2}\right) \\
& + \Big[\frac{3}{2}c_\Theta^4\Big((2e_t^2-6e_t^2\eta)\delta_{j,0} + (-e_t-\frac{9}{2}e_t^3+3e_t\eta+\frac{27}{2}e_t^3\eta)\left(\epsilon_j^{-1u}+\epsilon_j^{1u}\right) \\
& + (6e_t^2-18e_t^2\eta)\left(\epsilon_j^{-2u}+\epsilon_j^{2u}\right) + (-\frac{3}{2}e_t^3+\frac{9}{2}e_t^3\eta)\left(\epsilon_j^{-3u}+\epsilon_j^{3u}\right)\Big) \\
& + \frac{1}{1-e_t^2}c_\Theta^2\Big((-108e_t^2+60e_t^4+4e_t^2\eta-4e_t^4\eta)\delta_{s-j,0} - (-54e_t+\frac{33}{2}e_t^3-\frac{9}{2}e_t^5 \\
& + 2e_t\eta+\frac{35}{2}e_t^3\eta-\frac{39}{2}e_t^5\eta)\left(\epsilon_j^{-1u}+\epsilon_j^{1u}\right) - (18e_t^2+6e_t^4-26e_t^2\eta+26e_t^4\eta)\left(\epsilon_j^{-2u}+\epsilon_j^{2u}\right) \\
& - (-\frac{9}{2}e_t^3-\frac{3}{2}e_t^5+\frac{13}{4}e_t^3\eta-\frac{13}{2}e_t^5\eta)\left(\epsilon_j^{-3u}+\epsilon_j^{3u}\right)\Big) \\
& + \frac{1}{1-e_t^2}\Big((105e_t^2-57e_t^4+5e_t^2\eta-5e_t^4\eta)\delta_{j,0} - (\frac{105}{2}e_t-\frac{87}{4}e_t^3+\frac{45}{4}e_t^5+\frac{5}{2}e_t\eta \\
& - \frac{7}{4}e_t^3\eta-\frac{3}{4}e_t^5\eta)\left(\epsilon_j^{-1u}+\epsilon_j^{1u}\right) + (9e_t^2+15e_t^4+e_t^2\eta-e_t^4\eta)\left(\epsilon_j^{-2u}+\epsilon_j^{2u}\right) \\
& - (\frac{9}{4}e_t^3+\frac{15}{4}e_t^5+\frac{1}{4}e_t^3\eta-\frac{1}{4}e_t^5\eta)\left(\epsilon_j^{-3u}+\epsilon_j^{3u}\right)\Big)\Big]X_{s-j}^{-3,0}\Big\},
\end{aligned}
\tag{B.2a}
$$

$$
\begin{aligned}
Q_s^{\times\,(1)} = \sum_{j=-\infty}^{\infty} \frac{i}{12}\Big\{ & \frac{1}{8} c_\Theta s_\Theta^2 (1-3\eta)\Big[(-256+346e_t^2-105e_t^4)\delta_{s-j,0} \\
& + (130e_t - 111e_t^3)\left(\epsilon_{s-j}^{-1u} + \epsilon_{s-j}^{1u}\right) + (-61e_t^2 + 42e_t^4)\left(\epsilon_{s-j}^{-2u} + \epsilon_{s-j}^{2u}\right) \\
& + 9e_t^3\left(\epsilon_{s-j}^{-3u} + \epsilon_{s-j}^{3u}\right) - \frac{3e_t^4}{2}\left(\epsilon_{s-j}^{-4u} + \epsilon_{s-j}^{4u}\right)\Big]\left(X_j^{-4,-4} - X_j^{-4,4}\right) \\
& + c_\Theta s_\Theta^2 (1-3\eta)\sqrt{1-e_t^2}\frac{3e_t}{4}\Big[(26-14e_t^2)\left(\epsilon_{s-j}^{-1u} - \epsilon_{s-j}^{1u}\right) - 9e_t\left(\epsilon_{s-j}^{-2u} - \epsilon_{s-j}^{2u}\right) \\
& + 2e_t^2\left(\epsilon_{s-j}^{-3u} - \epsilon_{s-j}^{3u}\right)\Big]\left(X_j^{-4,-4} + X_j^{-4,4}\right) \\
& + \frac{c_\Theta}{1-e_t^2}\Big[\Big(52 + 100e_t^2 - \frac{383}{4}e_t^4 - \frac{45}{4}e_t^6 - 4\eta - 48e_t^2\eta + \frac{183}{4}e_t^4\eta + \frac{25}{4}e_t^6\eta \\
& + s_\Theta^2\big(16 - \frac{49}{2}e_t^2 + \frac{19}{4}e_t^4 + \frac{15}{4}e_t^6 - 48\eta + \frac{147}{2}e_t^2\eta - \frac{57}{4}e_t^4\eta - \frac{45}{4}e_t^6\eta\big)\Big)\delta_{s-j,0} \\
& + \Big(-82e_t + \frac{1}{4}e_t^3 + \frac{171}{4}e_t^5 + 14e_t\eta + \frac{39}{4}e_t^3\eta - \frac{95}{4}e_t^5\eta + s_\Theta^2\big(-\frac{29}{2}e_t + \frac{97}{4}e_t^3 \\
& - \frac{39}{4}e_t^5 + \frac{87}{2}e_t\eta - \frac{291}{4}e_t^3\eta + \frac{117}{4}e_t^5\eta\big)\Big)\left(\epsilon_{s-j}^{-1u} + \epsilon_{s-j}^{1u}\right) \\
& + \Big(31e_t^2 - \frac{5}{2}e_t^4 - \frac{9}{2}e_t^6 - e_t^2\eta - \frac{3}{2}e_t^4\eta + \frac{5}{2}e_t^6\eta + s_\Theta^2\big(\frac{25}{4}e_t^2 - \frac{31}{4}e_t^4 + \frac{3}{2}e_t^6 - \frac{75}{4}e_t^2\eta \\
& + \frac{93}{4}e_t^4\eta - \frac{9}{2}e_t^6\eta\big)\Big)\left(\epsilon_{s-j}^{-2u} + \epsilon_{s-j}^{2u}\right) + \Big(-\frac{9}{4}e_t^3 - \frac{27}{4}e_t^5 - \frac{15}{4}e_t^3\eta + \frac{15}{4}e_t^5\eta \\
& + s_\Theta^2\big(-\frac{9}{4}e_t^3 + \frac{9}{4}e_t^5 + \frac{27}{4}e_t^3\eta - \frac{27}{4}e_t^5\eta\big)\Big)\left(\epsilon_{s-j}^{-3u} + \epsilon_{s-j}^{3u}\right) + \Big(\frac{3}{8}e_t^4 + \frac{9}{8}e_t^6 + \frac{5}{8}e_t^4\eta - \frac{5}{8}e_t^6\eta \\
& + s_\Theta^2\big(\frac{3}{8}e_t^4 - \frac{3}{8}e_t^6 - \frac{9}{8}e_t^4\eta + \frac{9}{8}e_t^6\eta\big)\Big)\left(\epsilon_{s-j}^{-4u} + \epsilon_{s-j}^{4u}\right)\Big]\left(X_j^{-4,-2} - X_j^{-4,2}\right) \\
& + \frac{c_\Theta\, e_t}{\sqrt{1-e_t^2}}\Big[\Big(6 - 42e_t^2 - 4\eta + 16e_t^2\eta + s_\Theta^2\big(-9 + 9e_t^2 + 27\eta - 27e_t^2\eta\big)\Big)\left(\epsilon_{s-j}^{-1u} - \epsilon_{s-j}^{1u}\right) \\
& + \Big(9e_t + 9e_t^3 - e_t\eta - 5e_t^3\eta + s_\Theta^2\big(3e_t - 3e_t^3 - 9e_t\eta + 9e_t^3\eta\big)\Big) \\
& \times \left(\epsilon_{s-j}^{-2u} - \epsilon_{s-j}^{2u}\right)\Big]\left(X_j^{-3,-2} + X_j^{-3,2}\right) \\
& + 3c_\Theta s_\Theta^2 (1-3\eta)e_t\sqrt{1-e_t^2}\left(\epsilon_j^{-1u} - \epsilon_j^{1u}\right)X_{s-j}^{-3,0}\Big\}.
\end{aligned}
\tag{B.2b}
$$

Bibliography

[1] Marc Favata. The gravitational-wave memory from eccentric binaries. *Phys. Rev. D*, 84(12):124013, December 2011.

[2] Albert Einstein. Die Feldgleichungen der Gravitation. *Sitzungsberichte der Preussischen Akademie der Wissenschaften zu Berlin*, pages 844–847, Nov 1915.

[3] Karl Schwarzschild. Über das Gravitationsfeld eines Massenpunktes nach der Einsteinschen Theorie. *Sitzungsberichte der Preussischen Akademie der Wissenschaften zu Berlin*, pages 189–196, Jan 1916.

[4] Albert Einstein. Die Grundlage der allgemeinen Relativitätstheorie. *Annalen der Physik*, 354(7):769–822, 1916.

[5] Albert Einstein. Näherungsweise Integration der Feldgleichungen der Gravitation. *Sitzungsberichte der Königlich Preussischen Akademie der Wissenschaften zu Berlin*, pages 688–696, 1916.

[6] B. P. Abbott, R. Abbott, T. D. Abbott, M. R. Abernathy, F. Acernese, K. Ackley, C. Adams, T. Adams, P. Addesso, R. X. Adhikari, and et al. GW150914: First results from the search for binary black hole coalescence with Advanced LIGO. *Phys. Rev. D*, 93(12):122003, June 2016.

[7] B. P. Abbott, R. Abbott, T. D. Abbott, M. R. Abernathy, F. Acernese, K. Ackley, C. Adams, T. Adams, P. Addesso, R. X. Adhikari, and et al. GW150914: The Advanced LIGO Detectors in the Era of First Discoveries. *Physical Review Letters*, 116(13):131103, April 2016.

[8] The Nobel Prize in Physics 2017. http://www.nobelprize.org/nobel_prizes/physics/laureates/2017, May 2018.

[9] J. Centrella, J. G. Baker, B. J. Kelly, and James R. van Meter. Black-hole binaries, gravitational waves, and numerical relativity. *Rev. Mod. Phys.*, 82:3069, 2010.

[10] Albert Einstein. Über Gravitationswellen. *Sitzungsberichte der Königlich Preussischen Akademie der Wissenschaften zu Berlin*, pages 154–167, 1918.

[11] Sean M. Carroll. *Spacetime and geometry: An introduction to general relativity.* San Francisco, USA: Addison-Wesley (2004) 513 p, 2004.

[12] A. Gopakumar and B. R. Iyer. Second post-newtonian gravitational wave polarizations for compact binaries in elliptical orbits. *Phys. Rev. D*, 65:084011, Mar 2002.

[13] Lawrence E. Kidder. Using full information when computing modes of post-newtonian waveforms from inspiralling compact binaries in circular orbit. *Phys. Rev. D*, 77:044016, Feb 2008.

[14] Y. Boetzel, A. Susobhanan, A. Gopakumar, A. Klein, and P. Jetzer. Solving post-Newtonian accurate Kepler equation. *Phys. Rev. D*, 96(4):044011, August 2017.

[15] T. Damour, P. Jaranowski, and G. Schäfer. Conservative dynamics of two-body systems at the fourth post-Newtonian approximation of general relativity. *Phys. Rev. D*, 93(8):084014, April 2016.

[16] R. M. Memmesheimer, A. Gopakumar, and G. Schäfer. Third post-newtonian accurate generalized quasi-keplerian parametrization for compact binaries in eccentric orbits. *Phys. Rev. D*, 70:104011, Nov 2004.

[17] P. A. Hansen. Über Gravitationswellen. *Abhandlungen der Mathematisch-Physischen Klasse der Königlich-Sächsischen Gesellschaft der Wissenschaften, Leipzig*, 2:181–281, 1855.

[18] G. E. O. Giacaglia. A note on hansen's coefficients in satellite theory. *Celestial mechanics*, 14(4):515–523, Dec 1976.

[19] Sławomir Breiter, Gilles Métris, and David Vokrouhlický. Generalized hansen coefficients. *Celestial Mechanics and Dynamical Astronomy*, 88(2):153–161, Feb 2004.

[20] Sergey Yu Sadov. Analytic properties of hansen coefficients. *Celestial Mechanics and Dynamical Astronomy*, 100(4):287–300, Apr 2008.

[21] S. Hughes. The computation of tables of hansen coefficients. *Celestial mechanics*, 25(1):101–107, Sep 1981.

[22] Richard L. Branham. Recursive calculation of hansen coefficients. *Celestial Mechanics and Dynamical Astronomy*, 49(2):209–217, Jun 1990.

[23] P. C. Bazavan, L. F. Barbulescu, and P. Cefola. On the computation of the hansen coefficients. *2014 16th International Symposium on Symbolic and Numeric Algorithms for Scientific Computing*, pages 117–121, Sept 2014.

[24] M. Tessmer and G. Schäfer. Full-analytic frequency-domain first-post-Newtonian-accurate gravitational wave forms from eccentric compact binaries. *Phys. Rev. D*, 82(12):124064, December 2010.

[25] T. Damour, A. Gopakumar, and B. R. Iyer. Phasing of gravitational waves from inspiralling eccentric binaries. *Phys. Rev. D*, 70(6):064028, September 2004.

[26] A. Klein, N. Cornish, and N. Yunes. Gravitational waveforms for precessing, quasicircular binaries via multiple scale analysis and uniform asymptotics: The near spin alignment case. *Phys. Rev. D*, 88:124015, Dec 2013.

[27] Y. B. Zel'dovich and A. G. Polnarev. Radiation of gravitational waves by a cluster of superdense stars. *Soviet Astronomy*, 18:17, August 1974.

[28] A. Burrows and J. Hayes. Pulsar recoil and gravitational radiation due to asymmetrical stellar collapse and explosion. *Phys. Rev. Lett.*, 76:352–355, Jan 1996.

[29] K. Kotake, K. Sato, and K. Takahashi. Explosion mechanism, neutrino burst and gravitational wave in core-collapse supernovae. *Reports on Progress in Physics*, 69(4):971, 2006.

[30] M. B. Davies, A. King, S. Rosswog, and G. Wynn. Gamma-ray bursts, supernova kicks, and gravitational radiation. *The Astrophysical Journal Letters*, 579(2):L63, 2002.

[31] N. Sago, K. Ioka, T. Nakamura, and R. Yamazaki. Gravitational wave memory of gamma-ray burst jets. *Phys. Rev. D*, 70:104012, Nov 2004.

[32] T. Hiramatsu, K. Kotake, H. Kudoh, and A. Taruya. Gravitational wave background from neutrino-driven gamma-ray bursts. *Monthly Notices of the Royal Astronomical Society*, 364(3):1063–1068, 2005.

[33] K. Kotake, W. Iwakami, N. Ohnishi, and S. Yamada. Stochastic nature of gravitational waves from supernova explosions with standing accretion shock instability. *The Astrophysical Journal Letters*, 697(2):L133, 2009.

[34] R. Epstein. The generation of gravitational radiation by escaping supernova neutrinos. *Astrophysical Journal*, 223:1037–1045, August 1978.

[35] C. D. Ott. TOPICAL REVIEW: The gravitational-wave signature of core-collapse supernovae. *Classical and Quantum Gravity*, 26(6):063001, March 2009.

[36] Kip S. Thorne. Gravitational-wave bursts with memory: The christodoulou effect. *Phys. Rev. D*, 45:520–524, Jan 1992.

[37] Demetrios Christodoulou. Nonlinear nature of gravitation and gravitational-wave experiments. *Phys. Rev. Lett.*, 67:1486–1489, Sep 1991.

[38] L. Blanchet and T. Damour. Hereditary effects in gravitational radiation. *Phys. Rev. D*, 46:4304–4319, Nov 1992.

[39] P. N. Payne. Smarr's zero-frequency-limit calculation. *Phys. Rev. D*, 28:1894–1897, Oct 1983.

[40] C. M. Will and A. G. Wiseman. Gravitational radiation from compact binary systems: Gravitational waveforms and energy loss to second post-newtonian order. *Phys. Rev. D*, 54:4813–4848, Oct 1996.

[41] Alan G. Wiseman. Coalescing binary systems of compact objects to $(\text{post})^{\frac{5}{2}}$-newtonian order. iv. the gravitational wave tail. *Phys. Rev. D*, 48:4757–4770, Nov 1993.

[42] Richard A. Isaacson. Gravitational radiation in the limit of high frequency. ii. nonlinear terms and the effective stress tensor. *Phys. Rev.*, 166:1272–1280, Feb 1968.

[43] Kip S. Thorne. Multipole expansions of gravitational radiation. *Rev. Mod. Phys.*, 52:299–339, Apr 1980.

[44] Luc Blanchet. Gravitational radiation from post-newtonian sources and inspiralling compact binaries. *Living Reviews in Relativity*, 9(1):4, Jun 2006.

[45] L. Blanchet, G. Faye, B. R. Iyer, and S. Sinha. The third post-Newtonian gravitational wave polarizations and associated spherical harmonic modes for inspiralling compact binaries in quasi-circular orbits. *Classical and Quantum Gravity*, 25(16):165003, August 2008.

[46] A. G. Wiseman and C. M. Will. Christodoulou's nonlinear gravitational-wave memory: Evaluation in the quadrupole approximation. *Phys. Rev. D*, 44:R2945–R2949, Nov 1991.

[47] K. G. Arun, L. Blanchet, B. R. Iyer, and M. S. S. Qusailah. The 2.5PN gravitational wave polarizations from inspiralling compact binaries in circular orbits. *Classical and Quantum Gravity*, 21:3771–3801, August 2004.

[48] Marc Favata. Post-Newtonian corrections to the gravitational-wave memory for quasicircular, inspiralling compact binaries. *Phys. Rev. D*, 80(2):024002, July 2009.

[49] M. R. Spiegel and L. Liu. *Schaum's Mathematical Handbook of Formulas and Tables.* McGraw-Hill, New York, 1999. (see integral 18.32).

[50] Wolfram Research, Inc. Mathematica, Version 11.3. Champaign, IL, 2018.

[51] C. K. Mishra, K. G. Arun, and B. R. Iyer. Third post-Newtonian gravitational waveforms for compact binary systems in general orbits: Instantaneous terms. *Phys. Rev. D*, 91(8):084040, April 2015.

[52] E. A. Huerta, P. Kumar, B. Agarwal, D. George, H.-Y. Schive, H. P. Pfeiffer, R. Haas, W. Ren, T. Chu, M. Boyle, D. A. Hemberger, L. E. Kidder, M. A. Scheel, and B. Szilagyi. Complete waveform model for compact binaries on eccentric orbits. *Phys. Rev. D*, 95(2):024038, January 2017.

[53] G. Faye, S. Marsat, L. Blanchet, and B. R. Iyer. The third and a half-post-Newtonian gravitational wave quadrupole mode for quasi-circular inspiralling compact binaries. *Classical and Quantum Gravity*, 29(17):175004, September 2012.

[54] N. Yunes, K. G. Arun, E. Berti, and C. M. Will. Post-circular expansion of eccentric binary inspirals: Fourier-domain waveforms in the stationary phase approximation. *Phys. Rev. D*, 80:084001, Oct 2009.

[55] K. G. Arun, Luc Blanchet, Bala R. Iyer, and Siddhartha Sinha. Third post-newtonian angular momentum flux and the secular evolution of orbital elements for inspiralling compact binaries in quasi-elliptical orbits. *Phys. Rev. D*, 80:124018, Dec 2009.

[56] I. Kowalska, T. Bulik, K. Belczynski, M. Dominik, and D. Gondek-Rosinska. The eccentricity distribution of compact binaries. *Astronomy and Astrophysics*, 527:A70, March 2011.

[57] Thibault Damour. Introductory Lectures on the Effective One Body Formalism. *International Journal of Modern Physics A*, 23:1130–1148, 2008.

[58] Marc Favata. The gravitational-wave memory effect. *Classical and Quantum Gravity*, 27(8):084036, April 2010.

[59] Marc Favata. Gravitational-wave memory revisited: Memory from the merger and recoil of binary black holes. In *Journal of Physics Conference Series*, volume 154 of *Journal of Physics Conference Series*, page 012043, March 2009.

[60] E. Berti, V. Cardoso, and C. M. Will. Gravitational-wave spectroscopy of massive black holes with the space interferometer lisa. *Phys. Rev. D*, 73:064030, Mar 2006.

[61] Laser Interferometer Space Antenna (LISA). http://lisa.nasa.gov/, May 2018.

[62] L. Barack and C. Cutler. LISA capture sources: Approximate waveforms, signal-to-noise ratios, and parameter estimation accuracy. *Phys. Rev. D*, 69(8):082005, April 2004.

[63] Marc Favata. Nonlinear Gravitational-Wave Memory from Binary Black Hole Mergers. *The Astrophysical Journal Letters*, 696:L159–L162, May 2009.